Chemistry Research Journal, 2022, 7(6):52-83
Available online www.chemrj.org

Research Article

ISSN: 2455-8990
CODEN(USA): CRJHA5

Electronic structure and D_2, 5-HT_{1A}, 5-HT_{2A} and H_3 receptor affinities of some multi-target heterocycle piperazine derivatives. A DFT and FQSAR study

Juan S. Gómez-Jeria*, Matías Pinto-Saldaña

Quantum Pharmacology Unit, Laboratory of Theoretical Chemistry, Department of Chemistry, Faculty of Sciences, University of Chile. Las Palmeras 3425, Santiago 7800003, Chile
Correspondence to facien03@chile.cl (J.S.G.-J.)

Abstract The Klopman-Peradejordi-Gómez (KPG) QSAR method has been employed to find significant relationships between the electronic structure of a group of multi-target heterocycle piperazine derivatives and the D_2, 5-HT_{1A}, 5-HT_{2A} and H_3 receptor affinities. The electronic structure of all molecules was calculated at the B3LYP/6-311g(d,p) level using water as solvent. For each receptor affinity, statistically significant equations were obtained relating the variation of receptor affinity with the variation of the numerical values of a set of specific local atomic reactivity indices. For each case, drug-site receptor interactions were suggested. With this information, the partial 2D pharmacophores were suggested. The information generated here should help experimentalists to design new molecular structures.

Key words: Antipsychotics, heterocycle piperazine derivatives, KPG QSAR method, local atomic reactivity indices, haloperidol, clozapine, receptor affinity, D_2 receptor, 5-HT_{1A} receptor, 5-HT_{2A} receptor, H_3 receptor, schizophrenia

Introduction

Schizophrenia (SCZ) is a mental disorder that typically emerges in late adolescence or early adulthood and shows a marked heterogeneity in its clinical presentation, course and prognosis. Shrivastaba and De Sousa summarized this problem: "*There may be some patients in whom the disorder may be episodic, with long inter-episode recovery periods. There may be other patients in whom the disorder may have a relapsing and remitting course with multiple episodes and waxing and waning occurring annually. There are other patients who have complex symptoms that never abate and are present throughout the illness and where they are never symptom-free and have a chronic and almost progressive form of the disorder*" [1]. SCZ is characterized by a wide range of positive, negative and cognitive symptoms. Correll and Schooler mention that "*the negative symptom domain consists of five key constructs: blunted affect, alogia (reduction in quantity of words spoken), avolition (reduced goal-directed activity due to decreased motivation), asociality, and anhedonia (reduced experience of pleasure)*" [2]. Positive symptoms refer to the fact that there are signs (or symptoms) present rather than absent: delusions and irrational suspicions, a disorganized thought process and a confused manner of speaking, hallucinatory experiences and disorders of the motor system. Cognitive symptoms are related to attention and vigilance, processing speed, reasoning and problem solving, social cognition verbal learning and working memory [1-11].

The pharmacological approach to face SCZ is related to the discovery of the effects of chlorpromazine (see the work of Gomes and Grace for the historical aspects, Ref. [12], also [11, 13-15]). This molecule belongs to the group called first-generation antipsychotics or typical antipsychotics together with haloperidol, loxapine, perphenazine and

fluphenazine. These antipsychotics block the dopamine D_2 receptor. It is alleged that 60-80% of D_2 receptors need to be occupied for produce an antipsychotic effect. First generation antipsychotics exhibit neurological side effects, such as Parkinson's disease like extrapyramidal symptoms (akathisia, dystonia, pseudoparkinsonism, and tardive dyskinesia) (from Kaczor et al., Ref. [16]. The second generation of antipsychotics conform a group of drugs introduced after the 1970s and are used to treat psychiatric disorders. Clozapine was the first member of this group. In second generation drugs, neurological side effects are diminished but these drugs have metabolic side effects leading to weight gain, metabolic syndrome and diabetes [16].

First and second generation antipsychotics tend to block receptors in the brain's dopamine pathways. Both groups of molecules have a large list of adverse effects [15]. In 2002, it was marketed the first partial dopamine agonist antipsychotic, called aripiprazole, which represents the prototype of the third-generation antipsychotics, having a high affinity and a low intrinsic activity as partial D_2 agonist and partial 5-HT_{1A} agonist. Some first generation, second and third generation antipsychotics, such as chlorprothixene, clozapine, olanzapine, quietiapine risperidone or aripiprazole are multi-target ligands exerting their action through interactions with a number of receptors [16].

As Kaczor et al. summarize, "*In the case of multifunctional ligands it is needed to balance the affinity to a number of targets, to reduce affinity to off-targets and to avoid pharmacokinetic problems resulting from high molecular weight of the compounds*" [16]. Evidence points to the need of having molecules exhibiting a certain blockade of the dopamine D_2 receptor, an activation of the 5-HT_{1A} serotonin receptor in the frontal cortex (to improve the negative symptoms and cognitive deficits) and behaving as an inverse agonists of the of 5-HT_{2A} serotonin receptor (to counteract the excessive D_2 receptor blockade for relieving extrapyramidal effects and augmenting the efficacy against negative symptoms). This has led to the synthesis of several groups of molecules behaving as multi-target drugs that can be of possible antipsychotic use [17-22]. Among them Gao et al. synthesized a group of multi-target heterocycle piperazine derivatives and tested their receptor affinity for a series of receptors (dopamine D_2, serotonin 5-HT_{1A}, 5-HT_{2A} and 5-HT_6, and histamine H_3 receptors) [17].

This paper presents the results of the hypothesis stating that the linear version of the Klopman-Peradejordi-Gómez (KPG) method is able to find formal relationships between the electronic structure and the receptor affinity for the above-mentioned molecules. This should provide useful information for the medicinal chemists to synthesize new molecules.

Methods, Models and Calculations

The Method

We employed the Klopman-Peradejordi-Gómez (KPG) linear method [23]. It relates a biological activity (BA) with electronic structure through a linear relationship. The actual version includes twenty local atomic reactivity indices per atom. The equation is [24]:

$$\log(BA)=a+b\log\left(M_D\right)+\sum_{o=1}^{subs}\rho_o+\sum_{i=1}^{Z}\left[e_iQ_i+f_iS_i^E+s_iS_i^N\right]+$$
$$+\sum_{i=1}^{Z}\sum_{m=(HOMO-2)^*,i}^{(HOMO)^*,i}\left[h_i\left(m\right)F_i(m^*)+j_i\left(m\right)S_i^E\left(m^*\right)\right]+$$
$$+\sum_{i=1}^{Z}\sum_{m'=(LUMO)^*,i}^{(LUMO+2)^*,i}\left[r_i\left(m'\right)F_i(m'^*)+t_i\left(m'\right)S_i^N\left(m'^*\right)\right]+$$
$$+\sum_{i=1}^{Z}\left[g_i\mu_i^*+k_i\eta_i^*+o_i\omega_i^*+z_i\zeta_i^*+w_jQ_i^{*,max}\right] \quad (1)$$

where a, b, e_i, f_i, s_i $h_i(m)$, $j_i(m)$, $r_i(m')$, $t_i(m')$, g_i, k_i, o_i, z_i and w_i are constants to be determined, M_D is the mass of the drug and ρ_o is the orientational effect of the o-th substituent. Q_j is the net charge of the atom j. S_j^E and S_j^N are, respectively, the total atomic electrophilic and the total atomic nucleophilic superdelocalizabilities of atom j. $F_j(m)$

and $F_j(m')$ are, respectively, the electron populations (or Fukui indices) of the occupied (m) and vacant (m′) Local Molecular Orbitals (MOs) localized on atom j. $S_j^E(m)$ is the electrophilic superdelocalizability of the m-th occupied local MO localized on atom j. The molecular orbitals carrying an asterisk are the Local Molecular Orbitals (LMO) of each atom. For atom p, the LMOs of p are all the molecular MOs having an electron population greater than 0.01e on p.

The last terms of Eq. 1 were derived within the Hartree-Fock scheme by J.S. G.-J. [25]. μ_j is the local atomic electronic chemical potential of atom j, η_j is the local atomic hardness of the atom j, ω_j is the local atomic electrophilicity of atom j, ς_j is the local atomic softness of the atom j and Q_j^{max} is the maximum amount of electronic charge that atom j can accept. They are not identical to the local atomic indices derived within Density Functional Theory because in our case they have the same units that the global equivalents (eV and not eV×e). Here, we have included the three highest occupied local MOs and the three lowest empty local MOs of each atom. More local MOs may be included in Eq. 1 if necessary. A mandatory condition that the linear system of equations 1 must satisfy to be solved is that each equation must have the same number of terms. This condition is satisfied only by selecting a set of atoms common to all the molecules. This is called the common skeleton. The number of atoms of this common skeleton defines the index Z of Eq. 1 [26]. The second mandatory condition is that we must have at least the same number of equations than the total number of indices of the common skeleton plus the other terms of Eq. 1. As no paper or papers publish data fulfilling this condition, we use linear multiple regression analysis (LMRA) to detect those indices associated with the variation of the values of the biological activity. This method has produced excellent results for many biological activities and receptors [27-36].

Selection of Molecules and Activities

The selected biological activities were the binding affinities for serotonin (5-HT_{1A} and 5-HT_{2A}), dopamine (D_2) and histamine (H_3) receptors of twenty-three molecules from a paper of Gao et al. [17]. All data is shown in Table 1 and Fig. 1.

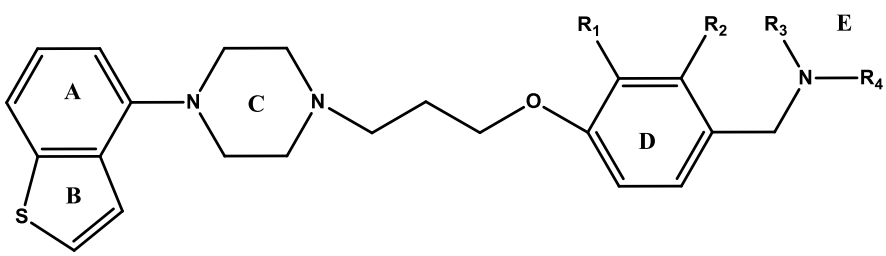

Figure 1: Heterocycle piperazine derivatives

Table 1: Heterocycle piperazine derivatives and receptor binding affinities

Mol.	R_1	R_2	NR_3R_4	log(K_i) (D_2)	log(K_i) (5-HT_{1A})	log(K_i) (5-HT_{2A})	log(K_i) (H_3)
1	$-CH_3$	$-H$		1.97	2.19	2.31	1.79
2	$-H$	$-CH_3$		1.98	2.21	2.44	1.83
3	$-F$	$-H$		2.00	2.19	2.41	1.97

4	$-H$	$-F$	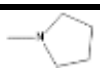	1.99	2.16	2.42	1.74
5	$-Cl$	$-H$	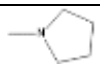	2.01	2.20	2.40	1.77
6	$-H$	$-Cl$	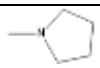	2.08	2.27	2.43	1.88
7	$-OCH_3$	$-H$	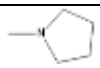	2.00	2.17	2.11	1.80
8	$-H$	$-H$	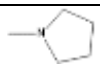	1.96	2.13	2.27	1.72
9	$-CH_3$	$-H$	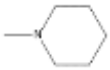	2.14	2.48	2.51	1.93
10	$-H$	$-CH_3$	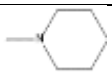	2.40	2.60	2.46	2.01
11	$-F$	$-H$	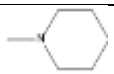	2.30	2.46	2.24	1.95
12	$-H$	$-F$	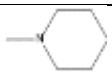	2.04	2.33	2.16	1.91
13	$-Cl$	$-H$	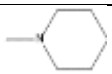	2.10	2.40	2.18	1.95
14	$-H$	$-Cl$	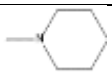	2.19	2.30	2.25	1.98
15	$-OCH_3$	$-H$	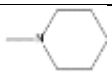	2.16	2.36	2.30	1.69
16	$-H$	$-H$	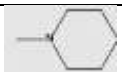	2.14	2.32	2.31	1.67
17	$-CH_3$	$-H$		1.96	1.16	1.09	1.75
18	$-F$	$-H$	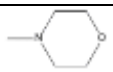	1.89	1.17	1.06	1.79
19	$-H$	$-F$	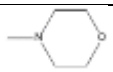	1.39	1.07	1.08	1.73
20	$-H$	$-Cl$	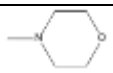	1.93	2.16	2.20	1.63

21	$-OCH_3$	$-H$	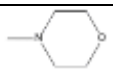	1.86	2.11	2.07	1.68
22	$-H$	$-H$	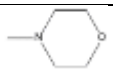	1.24	1.22	0.75	1.08
23	$-H$	$-H$	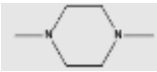	1.94	2.04	2.08	1.60

The next figures show the histogram of frequencies and the Box-Whiskers plot of values with median and quartile values for all data sets. Frequency histograms give general information about central tendency, range, shape and the variability of the data. The Box-Whiskers plot makes it easy to spot outliers. As the experimental results reported were obtained from three experiments, this plot should be only interpreted as a better vision of the homogeneity of the data distribution. Outliers and extreme values shown here reflect only the absence of the synthesis of molecules with a certain affinity in a given interval. Therefore, they should not be omitted from the initial set of values because there is no a scientific basis for doing this.

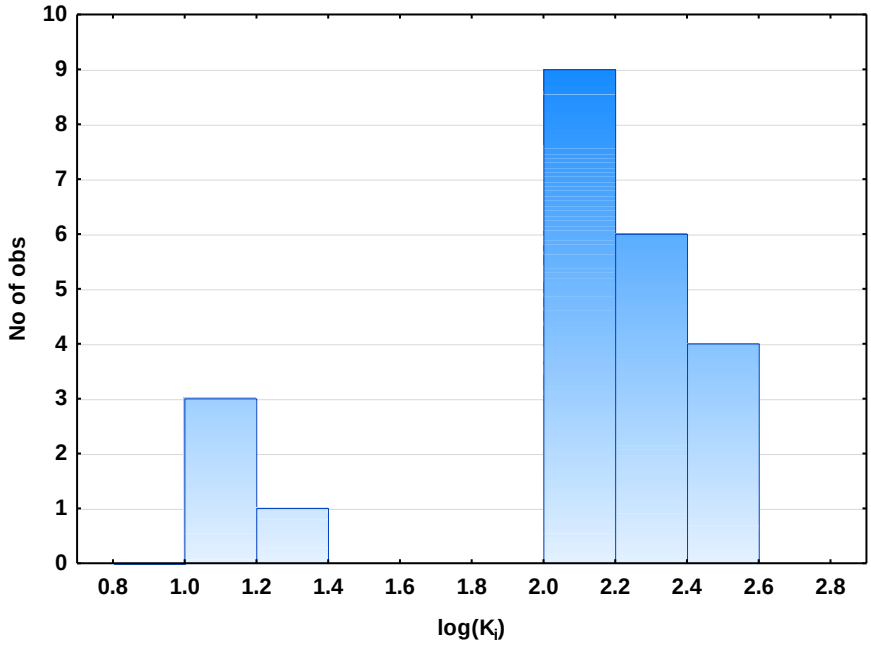

Figure 2: 5-HT$_{1A}$ receptor data. Histogram of frequencies

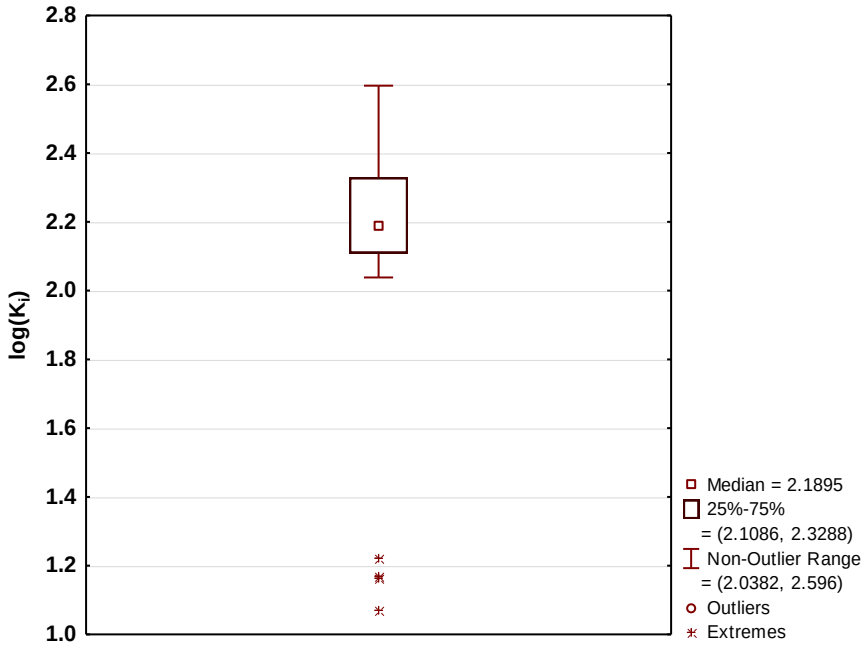

Figure 3: 5-HT$_{1A}$ receptor data. Box-Whiskers plot

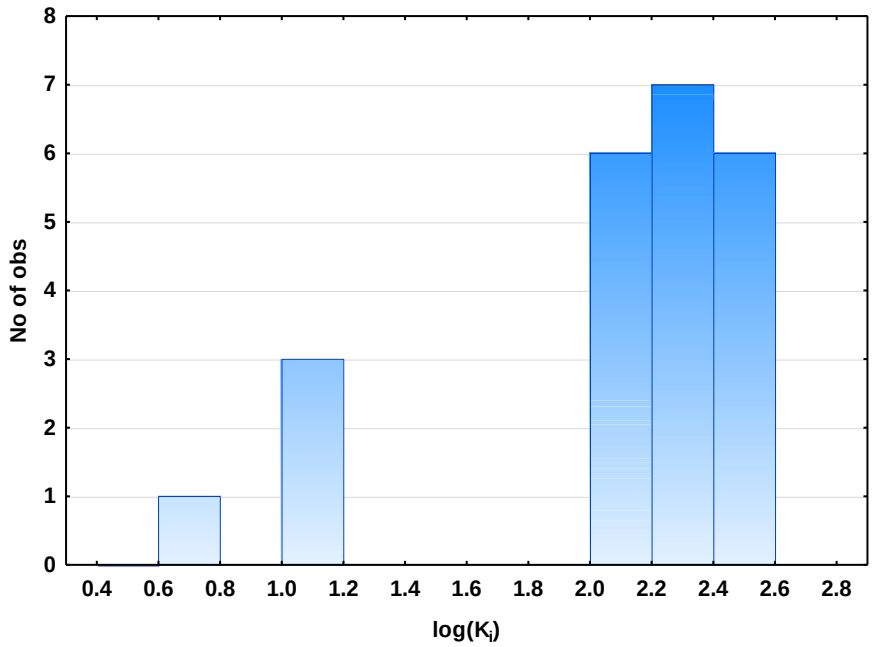

Figure 4: 5-HT$_{2A}$ receptor data. Histogram of frequencies

Figure 5: 5-HT$_{2A}$ receptor data. Box-Whiskers plot

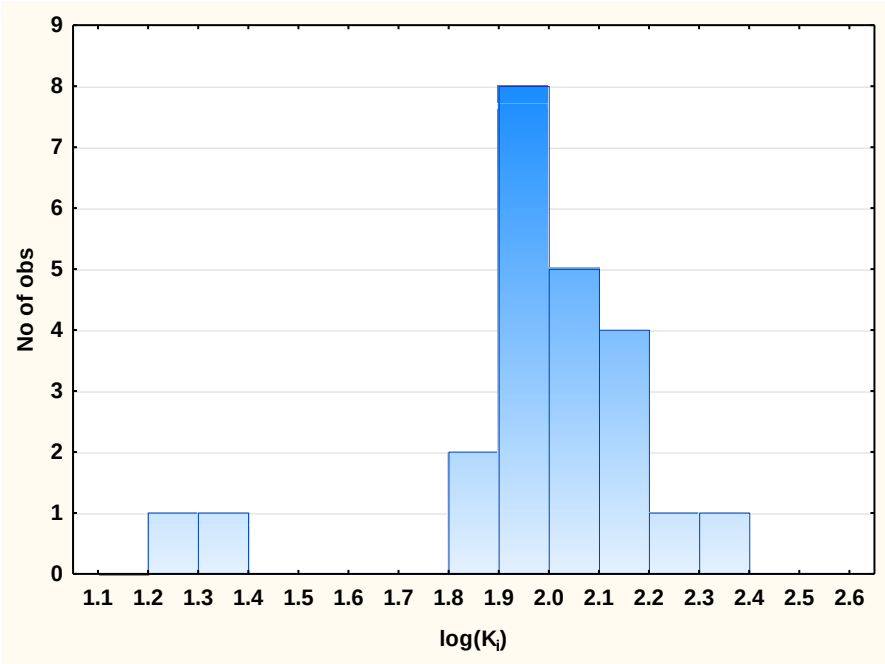

Figure 6: D$_2$ receptor data. Histogram of frequencies

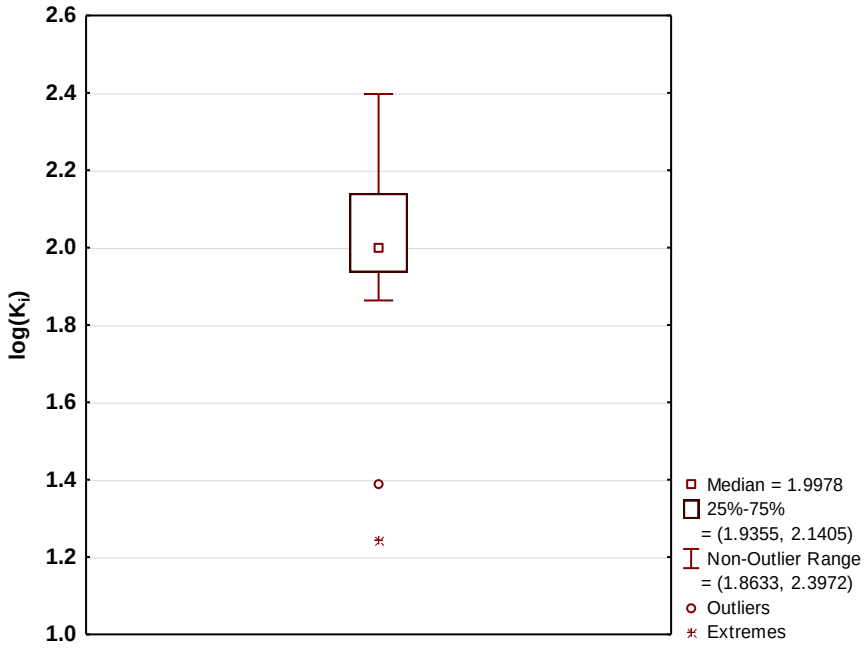

Figure 7: D_2 receptor data. Box-Whiskers plot

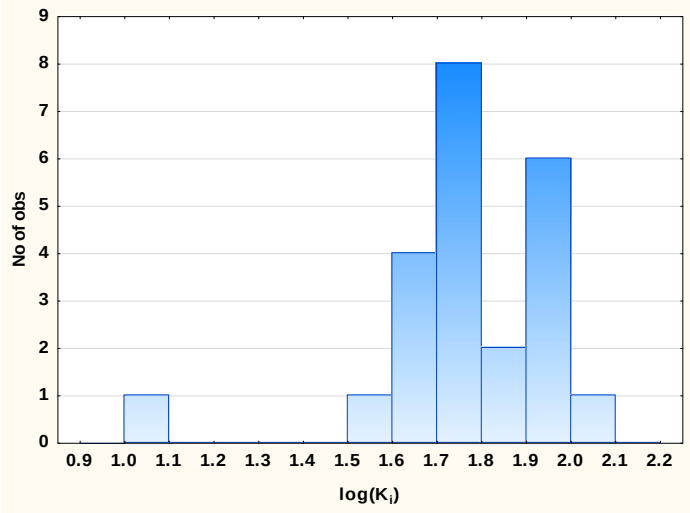

Figure 8: H_3 receptor data. Histogram of frequencies

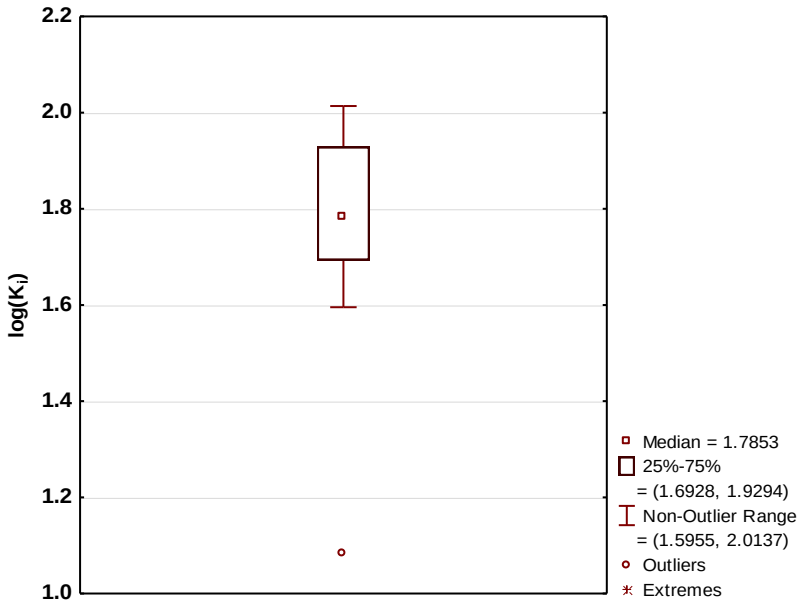

Figure 9: H_3 receptor data. Box-Whiskers plot

Electronic Structure Calculations

The electronic structure of all molecules was calculated within the Density Functional Theory (DFT) at the B3LYP/6-311g(d,p) level after full geometry optimization. Water was simulated as solvent for geometry optimization and single point calculations. The Gaussian 16 suite of programs was used [37]. The numerical values for the local atomic reactivity indices were obtained with the D-Cent-QSAR software [38]. All electron populations smaller than or equal to 0.01e were considered as being zero. Negative electron populations coming from Mulliken Population Analysis were corrected [39]. The Statistica software was used for LMRA [40]. The common skeleton used here is shown in Fig. 10.

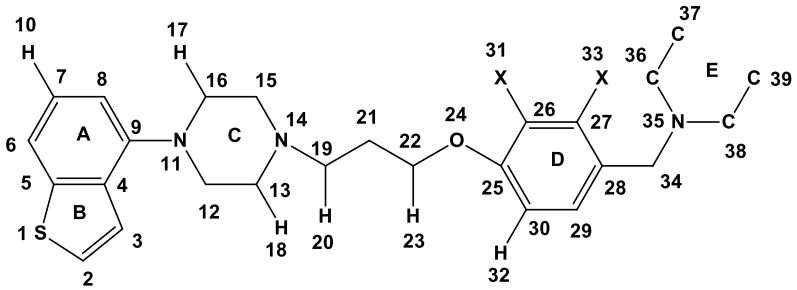

Figure 10: Common skeleton numbering

Results

Results for the 5-HT$_{1A}$ receptor affinity

The best equation obtained is:

$$\log(K_i)=-10.55-1.29S_{37}^{E}+0.65\omega_{18}+0.008S_{33}^{E} \quad (2)$$

with n=19, R=0.99, R^2=0.99, adj-R^2=0.98, F(3,15)=546.83 (p<0.000005) and SD=0.05. No outliers were detected and no residuals fall outside the ±2σ limits. Here, S_{37}^{E} is the total atomic electrophilic superdelocalizability of atom 37, ω_{18} is the local atomic electrophilicity of atom 18 and S_{33}^{E} is the total atomic electrophilic superdelocalizability of atom 33. Tables 2 and 3 show, respectively, the beta coefficients, the results of the t-test for significance of

coefficients and the matrix of squared correlation coefficients for the variables of Eq. 2. There are no significant internal correlations between independent variables. Figure 11 displays the plot of observed *vs.* calculated log(K_i).

Table 2: Beta coefficients and t-test for significance of coefficients in Eq. 2

Var.	Beta	t(15)	p-value
S_{37}^E	-1.09	-39.72	0.000000
ω_{18}	0.29	10.37	0.000000
S_{33}^E	0.10	3.81	0.002

Table 3: Matrix of squared correlation coefficients for the variables in Eq. 2

	S_{37}^E	ω_{18}	S_{33}^E
S_{37}^E	1		
ω_{18}	0.16	1	
S_{33}^E	0.01	0.04	1

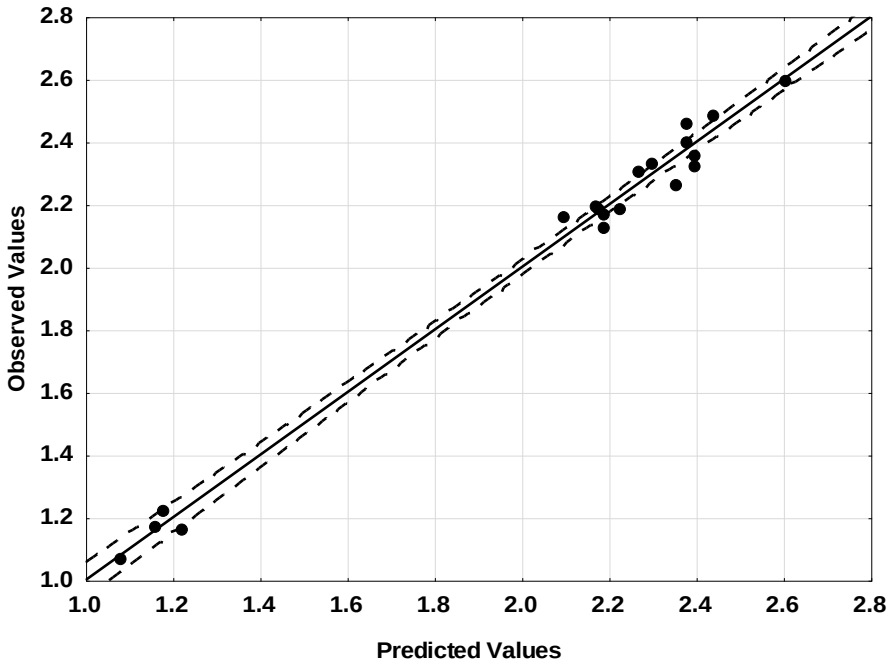

Figure 11: Plot of predicted vs. observed log(K_i) values (Eq. 2). Dashed lines denote the 95% confidence interval.

The associated statistical parameters of Eq. 2 indicate that this equation is statistically significant and that the variation of the numerical values of a group of three local atomic reactivity indices of atoms explains about 98% of the variation of log(K_i). Figure 11 shows that there is a good correlation of observed *versus* calculated values.

Remembering that Eq. 1 has a linear form but that the remaining terms contain non-linear terms we need to present, for each case, evidence supporting the hypothesis that a linear model is correct to be used in this case. A good regression analysis minimizes the residuals and it is expected that they be distributed as in a cloud showing no definite pattern or slope, centered (more or less) along of the horizontal axis (the x-axis is that of the values predicted by the regression equation) in a plot of predicted values vs. residuals scores. A random pattern indicates that the use of a linear model is correct. The plot of residuals versus deleted residuals shows the stability of the regression coefficients. No large discrepancies should appear between the residuals and the deleted residuals. Finally, we can use a normal probability plot of residuals to assess the normality of the distribution of a variable. If the observed residuals are distributed normally, they should fall on a straight line. Figures 12, 13 and 14 show, respectively, the plot of predicted values *vs.* residuals scores, the plot of residual *vs*. deleted residuals and the normal probability plot of residuals.

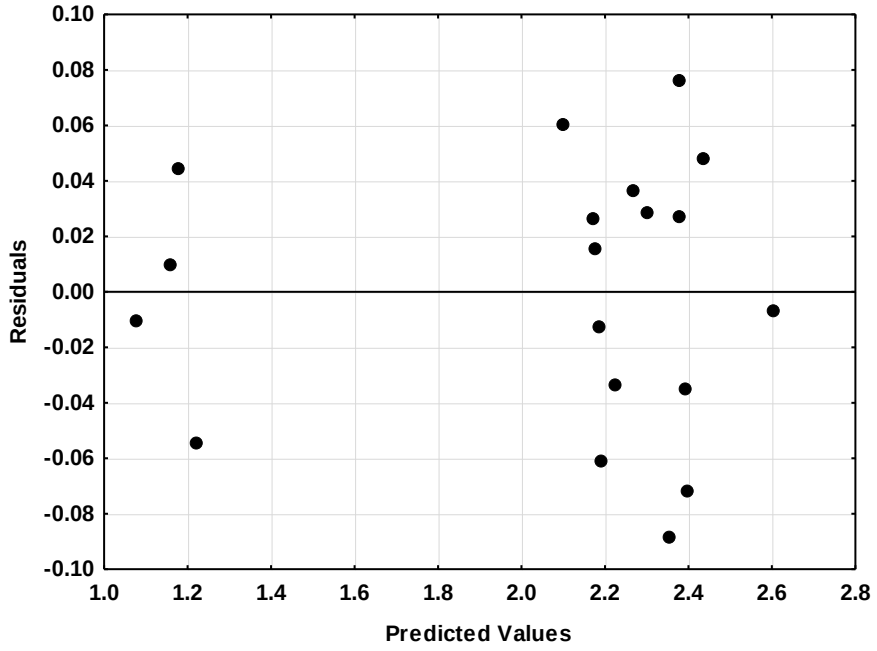

Figure 12: Plot of predicted values vs. residuals scores

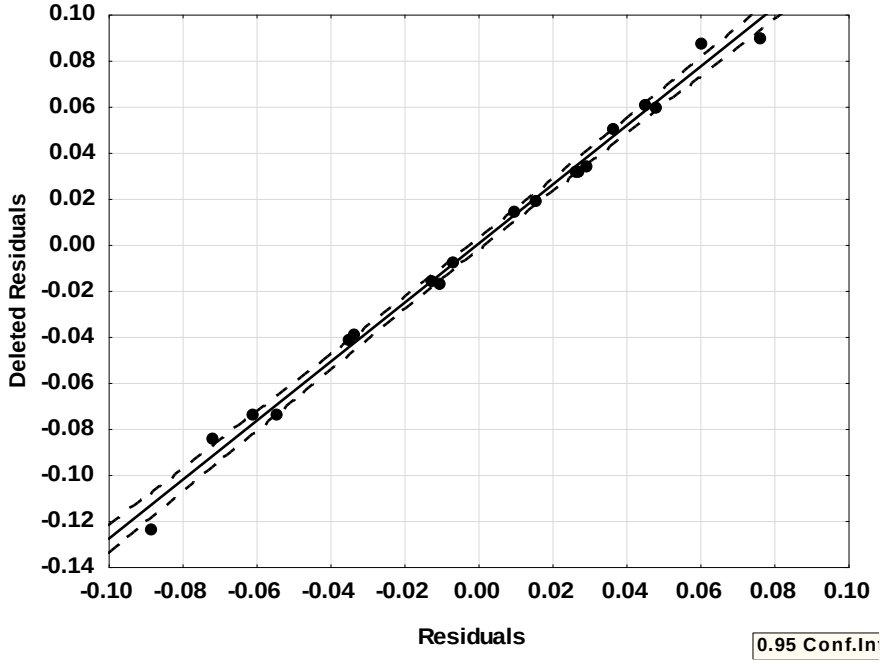

Figure 13: Plot of residual vs. deleted residuals

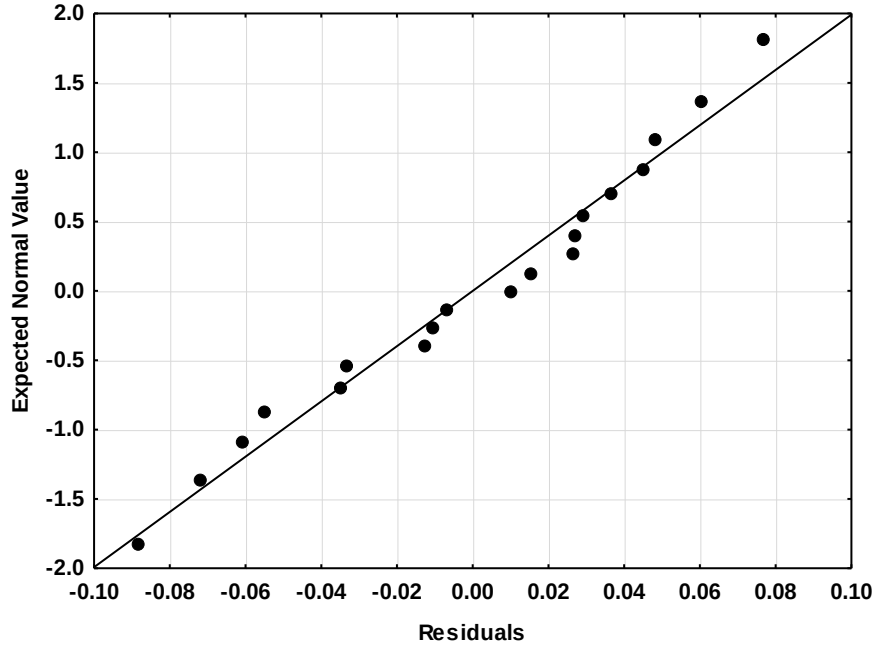

Figure 14: Normal probability plot of residuals

Figures 12, 13 and 14 provide support to state that the linear equation 2 is a good approximation to study the 5-HT_{1A} receptor affinity and that the regression coefficients are stable.

Results for the 5-HT_{2A} receptor affinity

The best equation obtained is:

$$\log(K_i)=2.12-0.53S^N_{37}(LUMO+1)^*+0.12S^N_{23}(LUMO+2)^*+0.24S^N_{22}(LUMO+1)^* \quad (3)$$

with n=19, R=0.98, R^2=0.97, adj-R^2=0.97, F(3,15)=243.09 (p<0.00000) and a standard deviation of 0.08. No outliers were detected and no residuals fall outside the ±2σ limits. Here, S_{37}^N(LUMO+1)* is the nucleophilic superdelocalizability of the second lowest empty local MO of atom 37, S_{23}^N(LUMO+2)* is the nucleophilic superdelocalizability of the third lowest empty local MO of atom 23 and S_{22}^N(LUMO+1)* is the nucleophilic superdelocalizability of the second lowest empty local MO of atom 22. Tables 4 and 5 show the beta coefficients, the results of the t-test for significance of coefficients and the matrix of squared correlation coefficients for the variables of Eq. 3. There are no significant internal correlations between independent variables (Table 5). Figure 15 displays the plot of observed *vs.* calculated values of log(K_i).

Table 4: Beta coefficients and t-test for significance of coefficients in Eq. 3

Var.	Beta	t(15)	p-value
S_{37}^N(LUMO+1)*	-0.89	-22.90	0.000000
S_{23}^N(LUMO+2)*	0.23	6.07	0.00002
S_{22}^N(LUMO+1)*	0.13	3.61	0.003

Table 5: Matrix of squared correlation coefficients for the variables in Eq. 3

	S_{37}^N(LUMO+1)*	**S_{23}^N(LUMO+2)***	**S_{22}^N(LUMO+1)***
S_{37}^N(LUMO+1)*	1		
S_{23}^N(LUMO+2)*	0.10	1	
S_{22}^N(LUMO+1)*	0.00	0.00	1

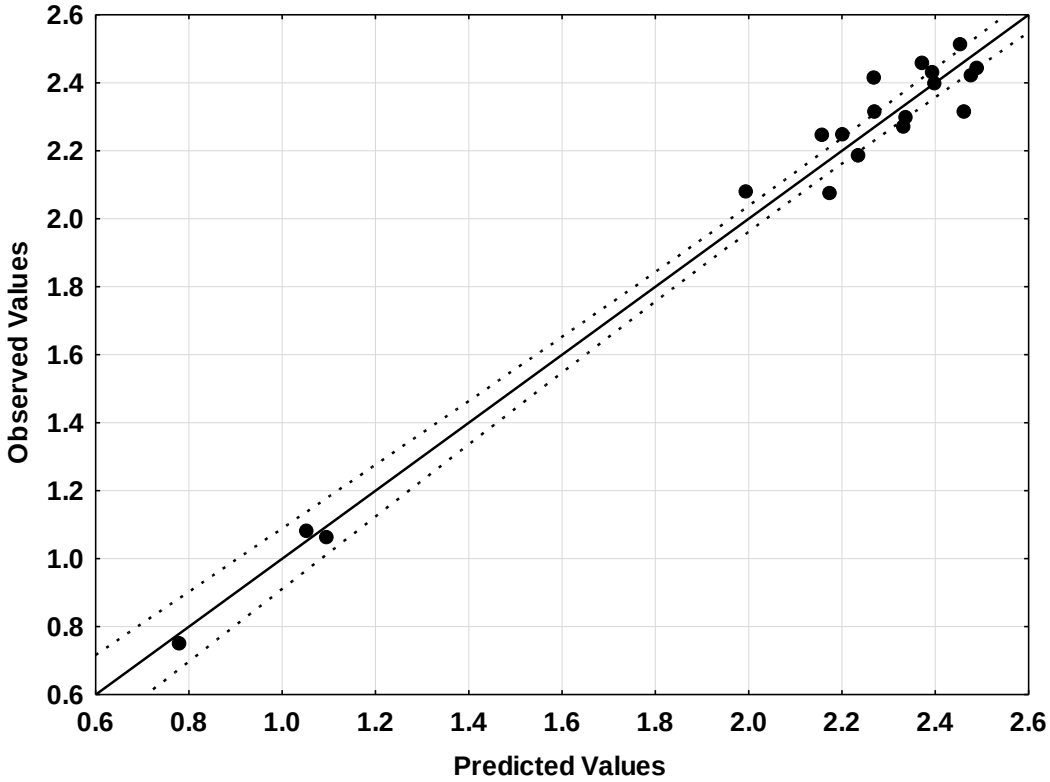

Figure 15: Plot of predicted vs. observed log(K_i) values (Eq. 3). Dashed lines denote the 95% confidence interval

The associated statistical parameters of Eq. 3 indicate that this equation is statistically significant and that the variation of the numerical values of a group of three local atomic reactivity indices of atoms constituting the common skeleton explains about 97% of the variation of log(K_i). Figure 15 shows that there is a good correlation of observed *versus* calculated log(K_i) values. Figures 16, 17 and 18 show, respectively, the plot of predicted values *vs.* residuals scores, the plot of residual *vs.* deleted residuals and the normal probability plot of residuals.

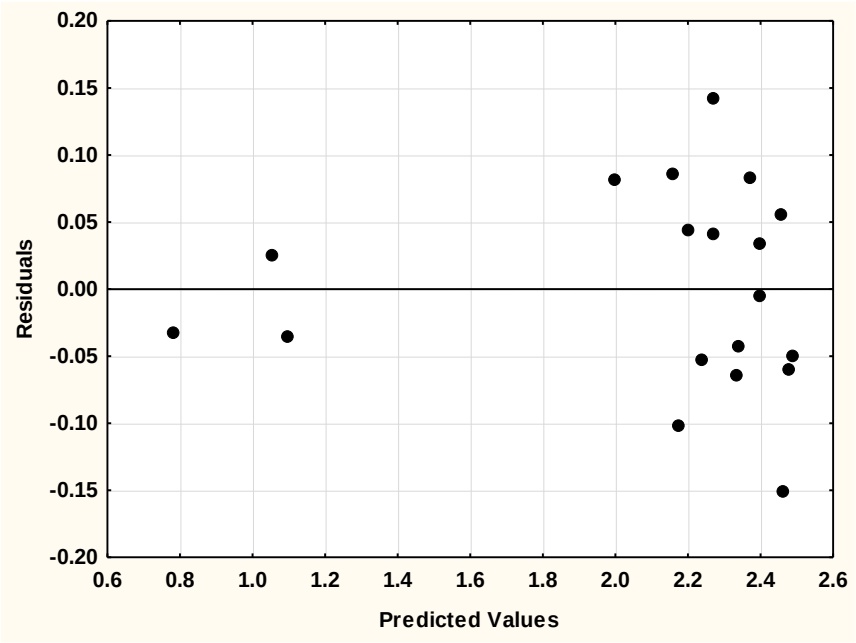

Figure 16: Plot of predicted values vs. residuals scores

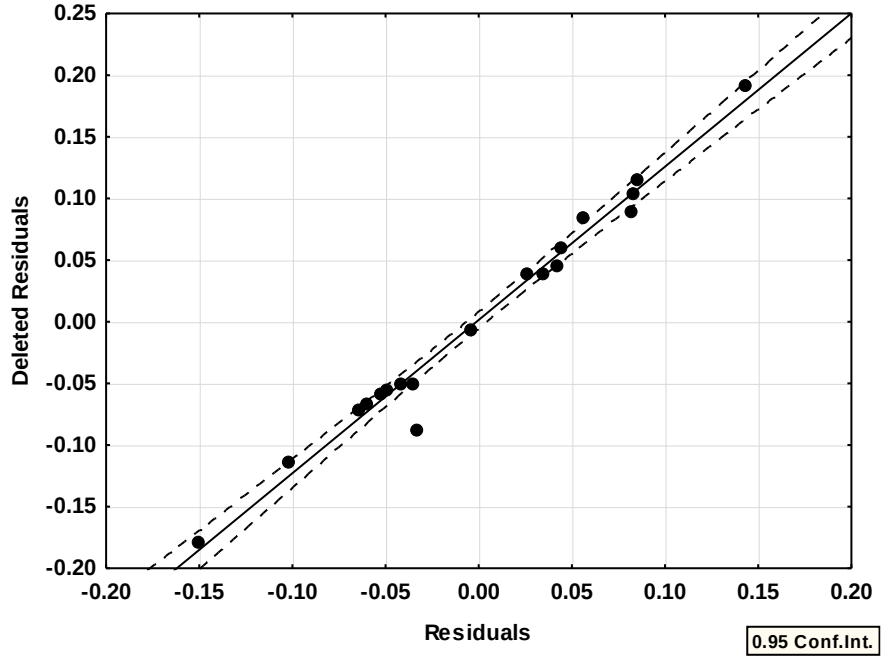

Figure 17: Plot of residual vs. deleted residuals

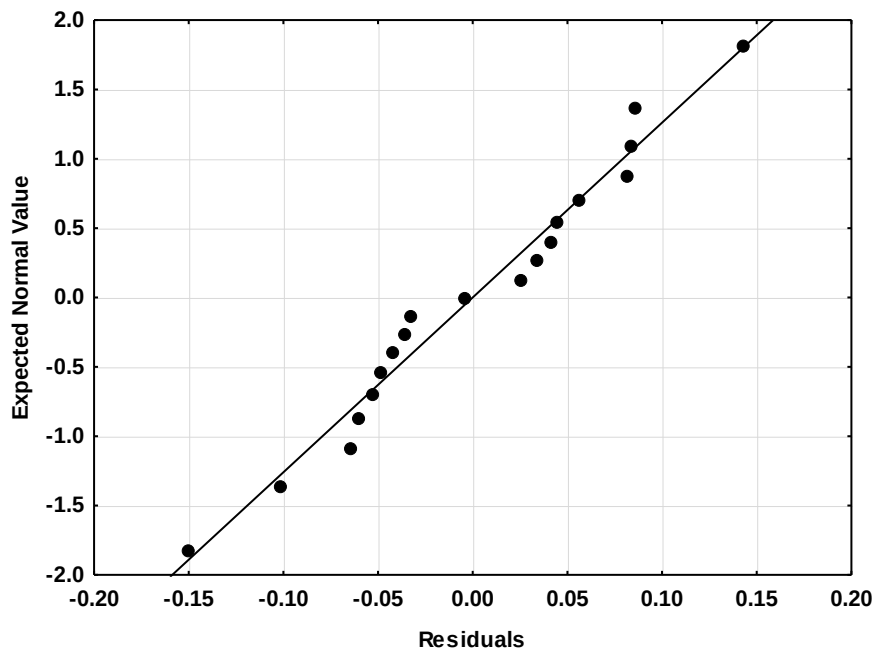

Figure 18: Normal probability plot of residuals

Figures 16, 17 and 18 provide support to state that the linear equation 3 is a good approximation to study the 5-HT_{2A} receptor affinity and that the regression coefficients are stable.

Results for the D_2 receptor affinity

The best equation obtained is:

$$\log(K_i)=3.29-0.26S_{37}^{N}(LUMO+1)^{*}-0.51S_{12}^{N}(LUMO+2)^{*}-0.09\eta_{22}^{*}-0.06S_{20}^{N}(LUMO+2)^{*} \quad (4)$$

with n=21, R=0.97, R^2=0.95, adj-R^2=0.93, F(4,16)=70.820 (p<0.00000) and SD=0.07. No outliers were detected and no residuals fall outside the ±2σ limits. Here, $S_{37}^{N}(LUMO+1)^{*}$ is the nucleophilic superdelocalizability of the

second lowest empty local MO of atom 37, S_{12}^{N}(LUMO+2)* is the nucleophilic superdelocalizability of the third lowest empty local MO of atom 12, η_{22}* is the local atomic hardness of atom 22 and S_{20}^{N}(LUMO+2)* is the nucleophilic superdelocalizability of the third lowest empty local MO of atom 20. Tables 6 and 7 show the beta coefficients, the results of the t-test for significance of coefficients and the matrix of squared correlation coefficients for the variables of Eq. 4. There are no significant internal correlations between independent variables (Table 7). Figure 19 displays the plot of observed *vs.* calculated values.

Table 6: Beta coefficients and t-test for significance of coefficients in Eq. 4

Var.	Beta	t(16)	p-value
S_{37}^{N}(LUMO+1)*	-0.83	-14.22	0.000000
S_{12}^{N}(LUMO+2)*	-0.52	-8.13	0.000000
η_{22}*	-0.35	-5.81	0.00003
S_{20}^{N}(LUMO+2)*	-0.26	-4.20	0.0007

Table 7: Matrix of squared correlation coefficients for the variables in Eq. 4

	S_{37}^{N}(LUMO+1)*	**S_{12}^{N}(LUMO+2)***	**η_{22}***	**S_{20}^{N}(LUMO+2)***
S_{37}^{N}(LUMO+1)*	1			
S_{12}^{N}(LUMO+2)*	0.00	1		
η_{22}*	0.00	0.06	1	
S_{20}^{N}(LUMO+2)*	0.00	0.13	0.01	1

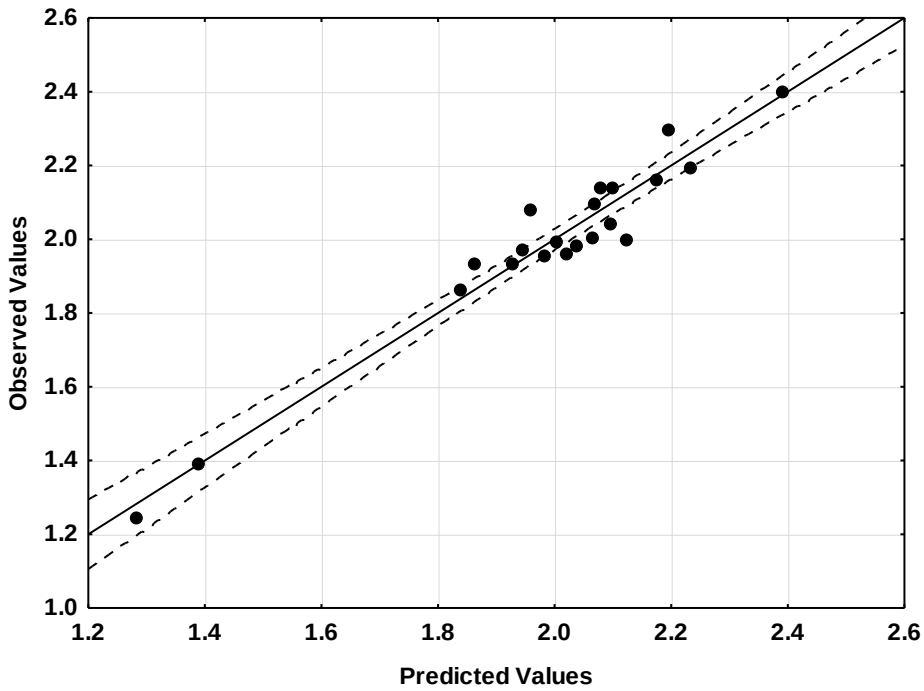

Figure 19: Plot of predicted vs. observed log(K_i) values (Eq. 4). Dashed lines denote the 95% confidence interval

The associated statistical parameters of Eq. 4 indicate that this equation is statistically significant and that the variation of the numerical values of a group of four local atomic reactivity indices of atoms constituting the common skeleton explains about 93% of the variation of log(K_i). Figure 19 shows that there is a good correlation of observed *versus* calculated values. Figures 20, 21 and 22 show, respectively, the plot of predicted values *vs.* residuals scores, the plot of residual *vs.* deleted residuals and the normal probability plot of residuals.

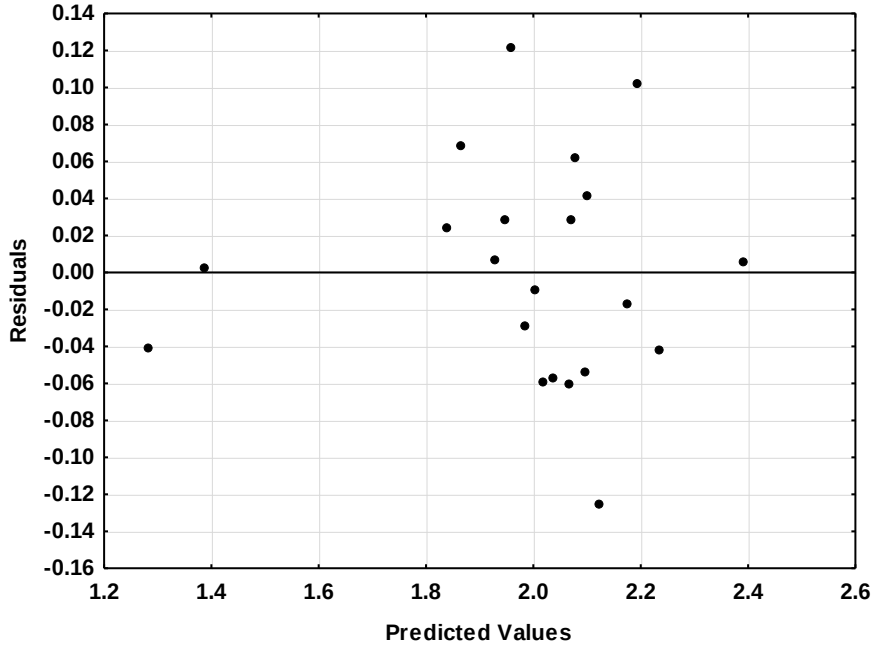

Figure 20: Plot of predicted values vs. residuals scores

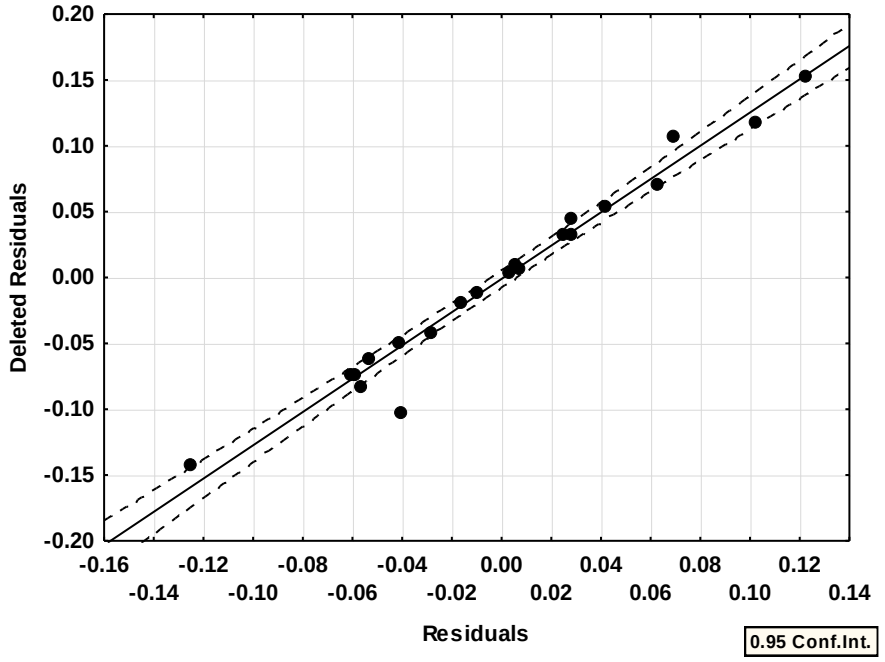

Figure 21: Plot of residual vs. deleted residuals

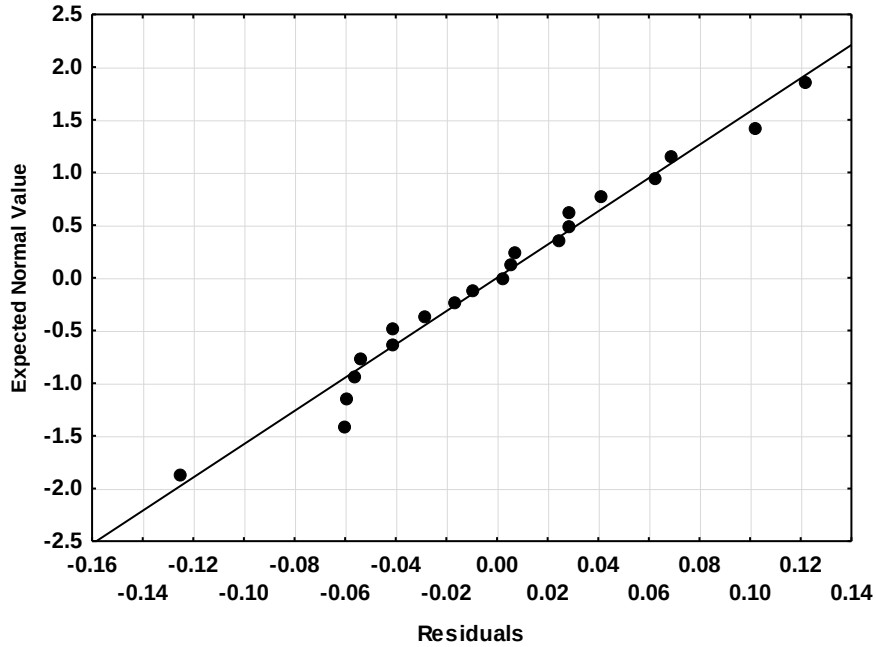

Figure 22: Normal probability plot of residuals

Figures 20, 21 and 22 provide support to state that the linear equation 4 is a good approximation to study the D_2 receptor affinity and that the regression coefficients are stable.

Results for the H_3 receptor affinity

The best equation obtained is:

$$\log(K_i)=1.70-0.17S^N_{39}(LUMO+2)^*-0.94S^E_{34}(HOMO)^*-$$
$$-0.28S^E_{37}(HOMO-2)^*-0.31S^N_{13}(LUMO+1)^* \quad (5)$$

with n=21, R= 0.95, R^2= 0.90, adj-R^2= 0.88, F(4,16)=36.278 (p<0.00000) and a standard error of estimate of 0.07. No outliers were detected and no residuals fall outside the ±2σ limits. Here, $S_{39}^N(LUMO+2)^*$ is the nucleophilic superdelocalizability of the third lowest empty local MO of atom 39, $S_{34}^E(HOMO)^*$ is the electrophilic superdelocalizability of the highest occupied local MO of atom 34, $S_{37}^E(HOMO-2)^*$ is the electrophilic superdelocalizability of the third highest occupied local MO of atom 37 and $S_{13}^N(LUMO+1)^*$ is the nucleophilic superdelocalizability of the second lowest empty local MO of atom 13. Tables 8 and 9 show the beta coefficients, the results of the t-test for significance of coefficients and the matrix of squared correlation coefficients for the variables of Eq. 5. There are no significant internal correlations between independent variables (Table 9). Figure 23 displays the plot of observed *vs.* calculated values.

Table 8: Beta coefficients and t-test for significance of coefficients in Eq. 5

Var.	Beta	t(16)	p-value
$S_{39}^N(LUMO+2)^*$	-0.75	-8.18	0.000000
$S_{34}^E(HOMO)^*$	-0.29	-3.25	0.005
$S_{37}^E(HOMO-2)^*$	-0.39	-4.65	0.0003
$S_{13}^N(LUMO+1)^*$	-0.34	-3.91	0.001

Table 9: Matrix of squared correlation coefficients for the variables in Eq. 5

	S_{39}^{N}(LUMO+2)*	S_{34}^{E}(HOMO)*	S_{37}^{E}(HOMO-2)*	S_{13}^{N}(LUMO+1)*
S_{39}^{N}(LUMO+2)*	1			
S_{34}^{E}(HOMO)*	0.15	1		
S_{37}^{E}(HOMO-2)*	0.07	0.01	1	
S_{13}^{N}(LUMO+1)*	0.01	0.06	0.05	1

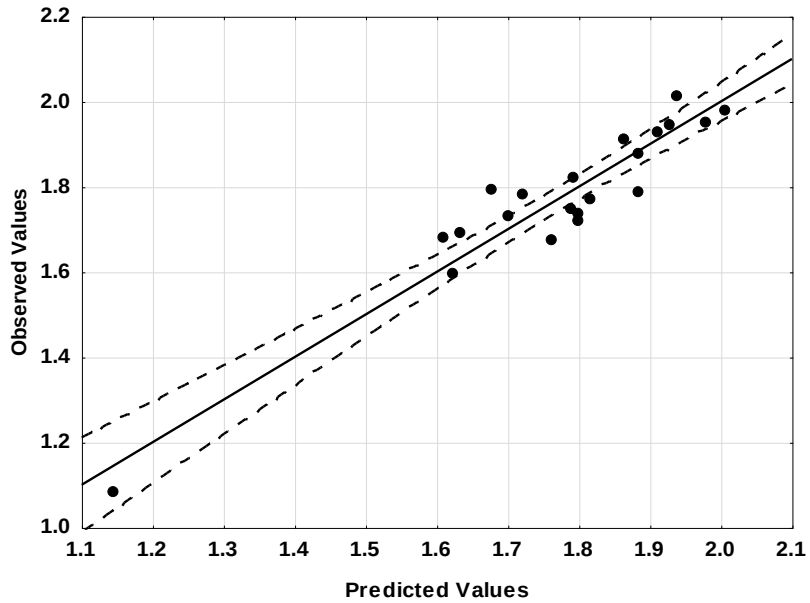

Figure 23: Plot of predicted vs. observed log(K_i) values (Eq. 5). Dashed lines denote the 95% confidence interval

The associated statistical parameters of Eq. 5 indicate that this equation is statistically significant and that the variation of the numerical values of a group of four local atomic reactivity indices of atoms constituting the common skeleton explains about 88% of the variation of log(K_i). Figure 23 shows that there is a good correlation of observed *versus* calculated values. Figures 24, 25 and 26 show, respectively, the plot of predicted values vs. residuals scores, the plot of residual vs. deleted residuals and the normal probability plot of residuals.

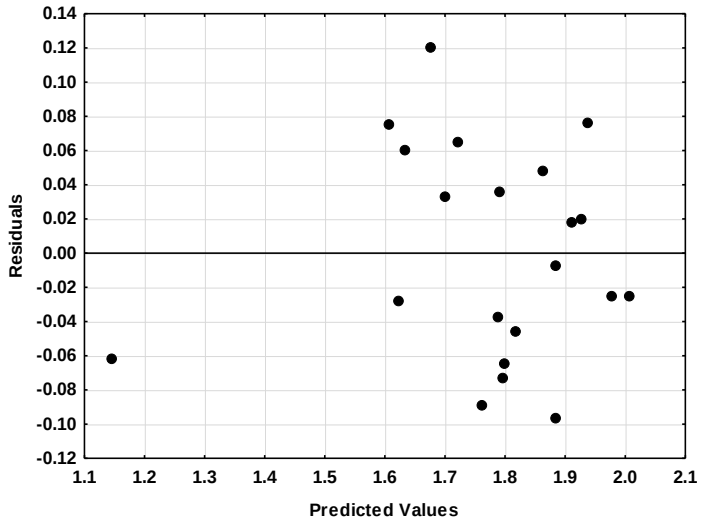

Figure 24: Plot of predicted values vs. residuals scores

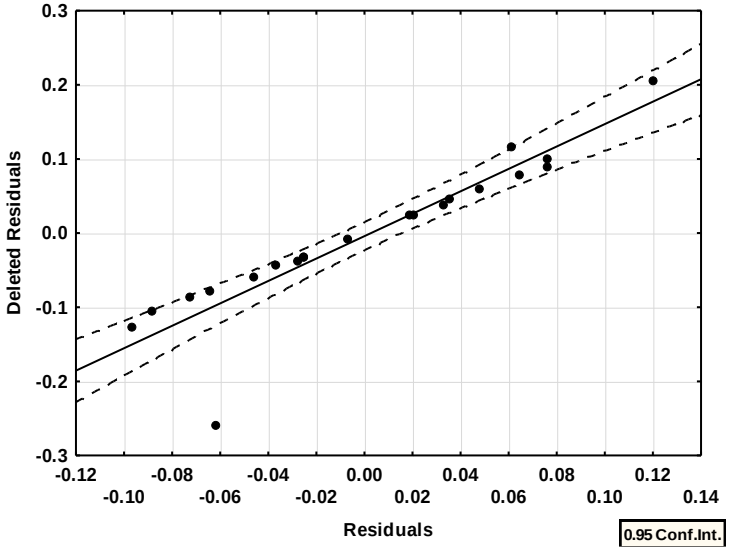

Figure 25: Plot of residual vs. deleted residuals

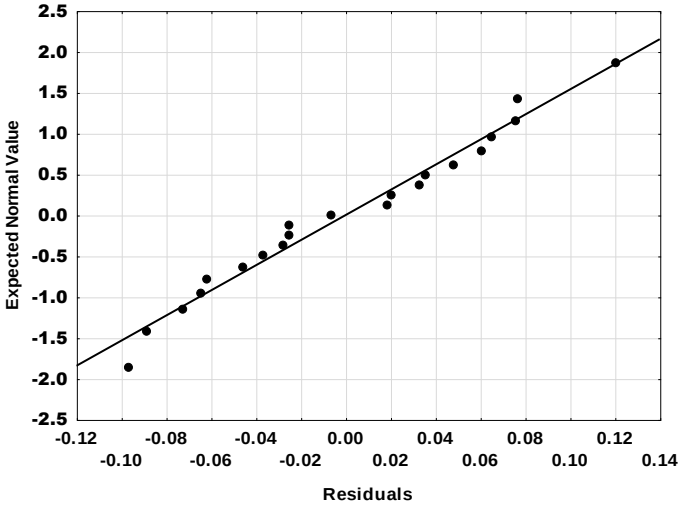

Figure 26: Normal probability plot of residuals

Figures 24, 25 and 26 provide support to state that the linear equation 5 is a good approximation to study the H_3 receptor affinity and that the regression coefficients are stable.

Local Molecular Orbitals

If a local atomic reactivity index of a inner occupied local MO (i.e., (HOMO-1)* and/or (HOMO-2)*) or of a higher vacant local MO ((LUMO+1)* and/or (LUMO+2)*) appears in an equation, this means that the remaining of the upper occupied local MOs (for example, if (HOMO-2)* appears, upper means (HOMO-1)* and (HOMO)*) or the remaining of the empty MOs (for example, if (LUMO+1)* appears, lower means the (LUMO)*) also contribute to the interaction. Their absence in the equation only means that the variation of their numerical values does not account for the variation of the numerical value of the biological property under analysis. Then, we worked with the hypothesis that any algebraic condition imposed on the numerical values of a reactivity index belonging to an inner occupied local MO or to an upper empty MO of a given atom, also holds for the corresponding local MOs having a lower energy.

Tables 10-12 list the local molecular orbitals of atoms appearing in Eq. 2 to 5 (lp denotes a lone pair).

Table 10: Local Molecular Orbitals of atoms 12, 13, 18 and 20.

Mol.	Atom 12 (C sp^3)	Atom 13 (C sp^3)	Atom 18 (H)	Atom 20 (H)
1 (121)	115σ119σ121σ-122σ124σ145σ	115σ119σ121σ-144σ145σ146σ	105σ107σ121σ-127σ128σ129σ	119σ120σ121σ-128σ129σ131σ
2 (121)	118σ120σ121σ-148σ149σ151σ	115σ120σ121σ-140σ142σ146σ	106σ108σ109σ-128σ129σ131σ	115σ120σ121σ-129σ130σ131σ
3 (121)	116σ120σ121σ-122σ124σ144σ	116σ120σ121σ-143σ145σ148σ	107σ109σ121σ-129σ132σ133σ	116σ120σ121σ-128σ129σ130σ
4 (121)	116σ120σ121σ-122σ124σ144σ	116σ120σ121σ-143σ145σ147σ	107σ110σ121σ-128σ132σ133σ	116σ120σ121σ-128σ130σ131σ
5 (125)	120σ124σ125σ-126σ129σ136σ	120σ124σ125σ-146σ150σ153σ	109σ112σ125σ-133σ134σ137σ	120σ124σ125σ-133σ134σ135σ
6 (125)	120σ124σ125σ-153σ154σ155σ	120σ124σ125σ-143σ144σ146σ	112σ113σ114σ-133σ136σ138σ	120σ124σ125σ-133σ134σ135σ
7 (125)	119σ123σ125σ-126σ127σ136σ	119σ123σ125σ-148σ150σ153σ	110σ112σ125σ-133σ135σ136σ	119σ123σ125σ-133σ134σ136σ
8 (117)	115σ116σ117σ-118σ120σ130σ	112σ115σ117σ-134σ141σ143σ	101σ103σ117σ-124σ125σ128σ	115σ116σ117σ-124σ125σ126σ
9 (125)	122σ123σ125σ-150σ153σ155σ	119σ123σ125σ-136σ144σ147σ	110σ111σ112σ-131σ132σ134σ	123σ124σ125σ-131σ132σ133σ
10 (125)	122σ123σ125σ-151σ153σ155σ	119σ123σ125σ-142σ144σ145σ	109σ112σ113σ-132σ133σ135σ	119σ123σ125σ-132σ133σ134σ
11 (125)	120σ124σ125σ-153σ154σ155σ	120σ124σ125σ-143σ145σ146σ	110σ112σ113σ-132σ135σ137σ	120σ124σ125σ-132σ134σ135σ
12 (125)	120σ124σ125σ-152σ153σ155σ	120σ124σ125σ-143σ145σ146σ	110σ112σ113σ-132σ135σ136σ	120σ124σ125σ-132σ134σ135σ
13 (129)	124σ128σ129σ-156σ157σ158σ	124σ128σ129σ-148σ149σ150σ	110σ113σ116σ-137σ140σ141σ	124σ128σ129σ-137σ139σ141σ
14 (129)	124σ128σ129σ-157σ158σ159σ	124σ128σ129σ-147σ148σ151σ	114σ115σ116σ-137σ140σ141σ	124σ128σ129σ-137σ138σ139σ
15 (129)	123σ127σ129σ-158σ159σ160σ	123σ127σ129σ-148σ151σ156σ	112σ114σ115σ-136σ137σ140σ	123σ127σ129σ-136σ137σ138σ
16 (121)	119σ120σ121σ-147σ148σ149σ	116σ119σ121σ-139σ141σ146σ	106σ107σ108σ-128σ131σ133σ	119σ120σ121σ-128σ129σ130σ
17 (125)	122σ123σ125σ-152σ156σ158σ	122σ123σ125σ-136σ144σ146σ	110σ112σ113σ-131σ132σ134σ	122σ123σ125σ-131σ132σ135σ
18 (125)	120σ123σ125σ-152σ153σ155σ	120σ123σ125σ-137σ142σ143σ	111σ113σ114σ-132σ135σ136σ	120σ123σ125σ-132σ134σ135σ
19 (125)	120σ123σ125σ-152σ153σ155σ	120σ123σ125σ-142σ145σ146σ	111σ113σ114σ-132σ135σ136σ	120σ123σ125σ-132σ134σ135σ
20 (129)	124σ127σ129σ-157σ158σ159σ	124σ127σ129σ-147σ149σ151σ	115σ116σ117σ-137σ139σ140σ	124σ127σ129σ-137σ139σ144σ
21 (129)	123σ126σ129σ-158σ159σ161σ	123σ126σ129σ-147σ148σ149σ	113σ115σ116σ-136σ137σ139σ	123σ126σ129σ-136σ137σ138σ
22 (121)	116σ119σ121σ-148σ149σ150σ	116σ119σ121σ-139σ141σ142σ	106σ108σ109σ-128σ130σ131σ	116σ119σ121σ-128σ129σ130σ
23 (125)	122σ124σ125σ-151σ153σ154σ	119σ124σ125σ-143σ146σ150σ	110σ112σ113σ-132σ135σ136σ	119σ124σ125σ-132σ133σ134σ

Table 11: Local Molecular Orbitals of atoms 22, 23, 30 and 33.

Mol	Atom 22 (C sp^3)	Atom 23 (H)	Atom 30 (C sp^2)	Atom 33
1 (121)	110σ111σ113σ-141σ145σ146σ	113σ118σ120σ-125σ128σ130σ	116π118π120π-123π125π145σ	104σ110σ111σ-128σ129σ130σ
2 (121)	111σ113σ120σ-140σ144σ147σ	111σ113σ118σ-125σ128σ129σ	116π118π120π-123π125π144σ	113σ116σ119σ-125σ155σ158σ
3 (121)	111σ112σ113σ-136σ138σ140σ	112σ113σ118σ-125σ129σ130σ	118π119π120π-123π125σ146π	104σ110σ119σ-128σ130σ131σ
4 (121)	111σ112σ113σ-134σ139σ141σ	112σ113σ118σ-123σ128σ130σ	113π115π118π-123π125π145σ	113π115π118π-123π125π140σ
5 (125)	115σ116σ117σ-131σ146σ150σ	115σ116σ122σ-128σ133σ134σ	119π122π123π-127π128π131σ	105σ113σ123σ-131σ133σ134σ
6 (125)	114σ116σ117σ-131σ146σ149σ	114σ117σ122σ-128σ133σ135σ	117π119π122π-127π128π146σ	119π122π123π-127lp128lp131σ
7 (125)	115σ116σ117σ-138σ144σ145σ	115σ117σ124σ-129σ133σ134σ	117π120π124π-128π129π146σ	105σ113σ122σ-132σ135σ138σ
8 (117)	106σ107σ109σ-138σ141σ143σ	107σ109σ114σ-121σ124σ125σ	114π115π116π-119π121π138σ	100σ106σ107σ-124σ125σ127σ
9 (125)	114σ115σ117σ-149σ151σ152σ	117σ122σ124σ-129σ132σ134σ	120π122π124π-127π129π148π	107σ109σ114σ-132σ133σ134σ
10 (125)	116σ117σ123σ-139σ144σ148σ	116σ117σ122σ-129σ132σ133σ	120π122π123π-127π129π144σ	117σ120σ124σ-129σ153σ160σ
11 (125)	115σ116σ117σ-138σ144σ145σ	116σ117σ122σ-129σ132σ133σ	122π123π124π-127π129σ145σ	107σ111σ123σ-133σ136σ137σ
12 (125)	115σ116σ117σ-138σ143σ145σ	116σ117σ122σ-127σ132σ134σ	119π122π124π-127π129π143σ	115π119π122π-127π129π137σ
13 (129)	118σ119σ120σ-135σ148σ150σ	118σ120σ126σ-132σ137σ139σ	123π126π127π-131π132π135σ	108σ114σ127σ-135σ137σ138σ
14 (129)	119σ120σ121σ-135σ151σ152σ	120σ121σ126σ-132σ137σ138σ	121π123π126π-131π132π150σ	123π126π127π-131lp132lp135σ
15 (129)	118σ119σ121σ-142σ148σ151σ	119σ121σ128σ-133σ136σ137σ	124π126π128π-132π133π148σ	114σ115σ126σ-132σ136σ137σ
16 (121)	110σ111σ113σ-134σ144σ145σ	111σ113σ118σ-125σ128σ130σ	115π118π120π-123π125π140σ	103σ109σ110σ-129σ132σ133σ
17 (125)	115σ116σ123σ-148σ149σ151σ	116σ122σ123σ-129σ132σ134σ	122π123π124π-127π129π144π	113σ114σ124σ-132σ133σ134σ
18 (125)	114σ115σ116σ-137σ138σ140σ	115σ116σ122σ-129σ132σ133σ	118π119π122π-127π129π145σ	108σ110σ112σ-133σ135σ136σ
19 (125)	114σ115σ116σ-138σ142σ144σ	115σ116σ122σ-127σ132σ133σ	116π119π122π-127π129π143σ	115π119π122π-127π129π134σ
20 (129)	117σ119σ120σ-135σ142σ147σ	119σ120σ126σ-132σ137σ138σ	120π123π126π-131π132π148σ	120π123π126π-131lp132lp135σ
21 (129)	118σ119σ120σ-142σ148σ150σ	119σ120σ127σ-133σ136σ138σ	124π127π128π-132π133π150σ	115σ116σ128σ-132σ136σ137σ
22 (121)	110σ111σ112σ-134σ145σ148σ	111σ112σ118σ-125σ128σ130σ	118π119π120π-123π125π139σ	102σ104σ110σ-129σ131σ132σ
23 (125)	114σ115σ116σ-139σ145σ146σ	115σ116σ121σ-129σ132σ134σ	121π122π124π-127π129π152σ	107σ108σ115σ-133σ134σ135σ

Table 12: Local Molecular Orbitals of atoms 34, 37 and 39.

Mol.	Atom 34 (C sp^3)	Atom 37 (C sp^3)	Atom 39 (C sp^3)
1 (121)	118σ119σ120σ-123σ125σ151σ	110σ112σ113σ-137σ138σ144σ	110σ112σ113σ-140σ142σ143σ
2 (121)	113σ118σ119σ-125σ145σ151σ	111σ112σ113σ-147σ149σ154σ	111σ112σ113σ-140σ148σ154σ
3 (121)	113σ118σ119σ-123σ125σ149σ	111σ112σ113σ-143σ146σ155σ	111σ112σ113σ-141σ142σ155σ
4 (121)	113σ118σ119σ-125σ152σ154σ	110σ112σ113σ-146σ155σ156σ	110σ112σ113σ-150σ156σ158σ
5 (125)	117σ122σ123σ-127σ128σ131σ	114σ115σ116σ-142σ149σ151σ	114σ115σ116σ-144σ145σ162σ
6 (125)	117σ122σ123σ-128σ131σ158σ	115σ116σ117σ-141σ150σ151σ	115σ116σ117σ-158σ162σ166σ
7 (125)	117σ122σ124σ-128σ156σ157σ	115σ116σ117σ-148σ149σ151σ	115σ116σ117σ-144σ145σ147σ
8 (117)	114σ115σ116σ-121σ146σ150σ	106σ108σ109σ-142σ154σ155σ	106σ108σ109σ-135σ137σ139σ
9 (125)	122σ123σ124σ-127σ129σ153σ	116σ117σ122σ-147σ157σ159σ	115σ116σ117σ-147σ148σ150σ
10 (125)	117σ122σ124σ-129σ153σ154σ	116σ117σ124σ-149σ153σ159σ	116σ117σ124σ-148σ151σ159σ
11 (125)	117σ122σ123σ-127σ129σ150σ	116σ117σ123σ-146σ152σ157σ	116σ117σ123σ-146σ149σ158σ
12 (125)	117σ122σ123σ-129σ144σ156σ	116σ117σ123σ-146σ147σ156σ	116σ117σ123σ-146σ147σ148σ
13 (129)	121σ126σ127σ-131σ132σ135σ	120σ121σ127σ-150σ162σ163σ	120σ121σ127σ-150σ151σ163σ
14 (129)	121σ126σ127σ-132σ135σ161σ	120σ121σ127σ-150σ152σ161σ	120σ121σ127σ-152σ153σ159σ
15 (129)	121σ126σ128σ-132σ159σ162σ	120σ121σ126σ-150σ154σ162σ	120σ121σ126σ-153σ160σ161σ
16 (121)	118σ119σ120σ-125σ153σ154σ	111σ112σ113σ-142σ153σ154σ	111σ112σ113σ-142σ144σ149σ
17 (125)	115σ116σ124σ-127σ129σ155σ	116σ118σ124σ-137σ147σ148σ	116σ118σ124σ-147σ148σ150σ
18 (125)	116σ122σ124σ-127σ129σ147σ	116σ118σ124σ-145σ147σ148σ	116σ118σ124σ-145σ147σ148σ
19 (129)	116σ122σ124σ-129σ151σ152σ	116σ118σ124σ-147σ148σ149σ	116σ118σ124σ-147σ148σ152σ
20 (129)	120σ126σ128σ-132σ135σ156σ	120σ122σ128σ-152σ153σ154σ	120σ122σ128σ-148σ150σ152σ
21 (129)	120σ127σ128σ-132σ151σ157σ	120σ122σ128σ-150σ151σ152σ	120σ122σ128σ-151σ152σ153σ
22 (121)	112σ118σ120σ-123σ125σ148σ	112σ114σ120σ-143σ144σ148σ	112σ114σ120σ-141σ143σ144σ
23 (125)	116σ121σ122σ-127σ129σ156σ	115σ121σ123σ-151σ156σ157σ	116σ121σ123σ-152σ156σ157σ

Discussion

Discussion of the results for the 5-HT_{1A} receptor affinity

Table 2 shows that the importance of variables in Eq. 2 is $S_{37}^E >> \omega_{18} > S_{33}^E$. Note that the electrophilic superdelocalizabilities always have negative numerical values and that the electrophilicity always has positive numerical values. The algebraic analysis of Eq. 2 shows that a high 5-HT_{1A} receptor affinity is associated with small (negative) numerical values for S_{37}^E, large (positive) numerical values for ω_{18} and with large negative values for S_{33}^E.

Atom 37 is a sp^3 carbon atom in ring E (see Fig.1 and Fig. 10). This atom is part of ring E that is a five- or six-membered ring. Note that in molecules 17-23 this atom is bonded to oxygen or nitrogen atoms. Table 12 shows that all local MOs have a σ nature. In all molecules the local (LUMO)* is energetically far from the molecular LUMO. The local (HOMO)* is quite close in energy to the molecular HOMO in some cases. A high 5-HT_{1A} receptor affinity is associated with small (negative) numerical values for S_{37}^E. Let us remember that:

$$S_{37}^{E} = \sum_{i=1}^{HOMO^*} \frac{F_{37}(i)^*}{E_i^*} \qquad (6)$$

where $F_{37}(i)^*$ is the electron population of MO i at atom 37 and E_i^* is the corresponding eigenvalue. Given that the highest occupied local MOs have energies closer to zero, they are the dominant terms in Eq. 6. Therefore, the only way to get small negative numerical values is by eliminating the localization of the higher occupied molecular MOs on atom 37, i.e. $(HOMO)_{37}^*$ should coincide with an inner occupied molecular MO. All this procedure will make C37 a very bad electron donor. For this reason, we suggest that this atom could be engaged in alkyl and/or alkyl-π interactions at a distance of about 5.5Å [26].

Atom 18 is a hydrogen atom attached to a sp^3 carbon atom C13 of the saturated ring C (Figs. 1 and 10). Note that C13 is directly bonded to the nitrogen atom N14. All local MOs of atom 18 have a σ nature (Table 10). A high 5-HT_{1A} receptor affinity is associated with large (positive) numerical values for ω_{18}. This index is defined as:

$$\omega_{18}^{*} = \frac{(\mu_{18}^{*})^2}{2\eta_{18}^{2}} \qquad (7)$$

where μ_{18}^* is the local atomic electronic chemical potential (ECP) of atom 18 and η_{18}^* is the local atomic hardness of the same atom. It describes the tendency of the atom to receive extra electronic charge together with its resistance to exchange charge with the medium. Large positive values for this index may be obtained by lowering the value of the local atomic hardness (i.e., diminishing the energy of the $HOMO_{18}$*-$LUMO_{18}$* gap), by raising the value of the ECP (i.e., by shifting downwards the $HOMO_{18}$*-$LUMO_{18}$* energy midpoint) or by both procedures at once. The inspection of Table 10 shows that this can be easily done by lowering the eigenvalue of the local $(LUMO)_{18}$*, making atom 18 more prone to interact with an electron-rich center. The N14-C13-H18 system fulfills the conditions to form a N14-C13-H18.....X (X=O, N, S) non-classical carbon hydrogen bond (3.8Å is the approximate distance between the partners).

Atom 33 is the first atom of the substituent attached to the sp^2 carbon atom C27 of ring D (Fig.10). Table 1 shows that these substituents can be H, Me, F or Cl. Table 11 shows that local frontier MOs can have a π or σ natures following the case. A high 5-HT_{1A} receptor affinity is associated with large negative values for S_{33}^E. Eq. 6 shows that these values are obtained by shifting the local (HOMO)* energy toward zero, making atom 33 a good electron donor. Therefore, the ideal situation will occur when the molecular HOMO is localized *only* on this atom. Considering the nature and position of atom 33, this ideal situation is highly improbable. Here we need to consider more than one interaction possibility. For fluorine and chlorine, we may think in F...O=C and Cl...O=C interactions (3.7Å). For the methyl group we may have alkyl and/or alkyl interactions (5.5Å), but a C-H...π interaction should not be discarded. Hydrogen could participate in a C-H...π interaction. These various suggestions indicate that, close to atom 33, there are two or more different interactions sites. All the suggestions are displayed in the partial 2D pharmacophore of Fig. 27.

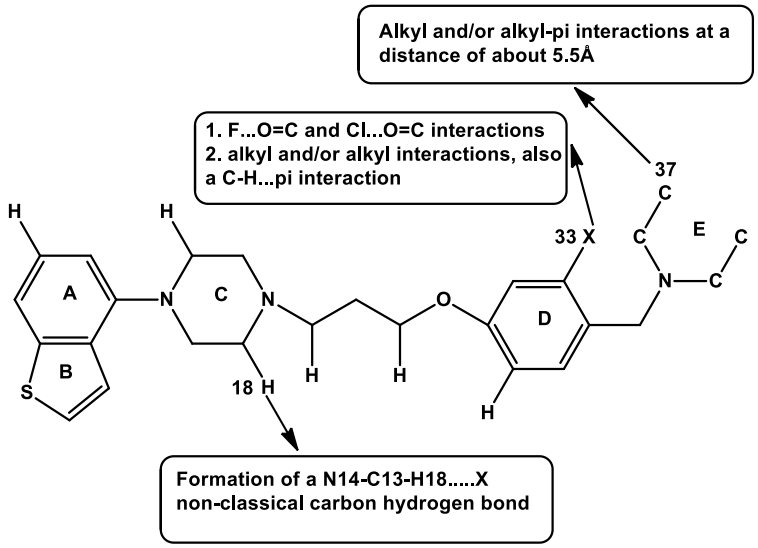

Figure 27: Partial 2D pharmacophore for 5-HT$_{1A}$ receptor affinity

Discussion of the results for the 5-HT$_{2A}$ receptor affinity

Table 4 shows that the importance of variables in Eq. 3 is S_{37}^{N}(LUMO+1)*>> S_{23}^{N}(LUMO+2)*> S_{22}^{N}(LUMO+1)*. A high 5-HT$_{2A}$ receptor affinity is associated with high positive numerical values for S_{37}^{N}(LUMO+1)* and small positive numerical values for S_{23}^{N}(LUMO+2)* and S_{22}^{N}(LUMO+1)*.

Atom 37 is a sp^3 carbon atom in ring E (see Fig.1 and Fig. 10). Table 12 shows that all local MOs have a sigma nature. High positive numerical values for S_{37}^{N}(LUMO+1)* are obtained by lowering the value of the (LUMO+1)*$_{37}$ eigenvalue, making this local MO more prone to interact with electron-rich regions. We suggest that this atom could be engaged in alkyl and/or alkyl-π interactions (distance of about 5.5Å).

Atom 23 is a hydrogen atom bonded to a carbon atom (C22) of the chain linking rings C and D (see Fig. 10). Note that C22 is bonded to an oxygen atom. All local molecular orbitals have a sigma character (Table 11). A high 5-HT$_{2A}$ receptor affinity is associated with small positive numerical values for S_{23}^{N}(LUMO+2)*. These values are obtained by shifting upwards the energy of this MO, making it a bad electron acceptor. On the other hand, Table 11 shows that the local (HOMO)*$_{23}$ is very close to the molecular HOMO. This last fact strongly suggests that atom 23 forms a O24-C22-H23.....X non-classical carbon hydrogen bond (at a distance of about 3.8Å between the partners). Note that in this case electrons flow from C22-H23 to X.

Atom 22 is a carbon atom in the chain linking rings C and D (see Fig. 10). All local molecular orbitals have a sigma character (Table 11). Small positive numerical values for S_{22}^{N}(LUMO+1)* are associated with high receptor affinity. With the same logic employed for atom 23, atom 22 should be a bad electron acceptor (it is also bonded to the more electronegative atom O24). For this atom we have two possible interactions. The first one is cooperating in the O24-C22-H23.....X non-classical carbon hydrogen bond. The second one is an alkyl interaction. All the suggestions are displayed in the partial 2D pharmacophore of Fig. 28.

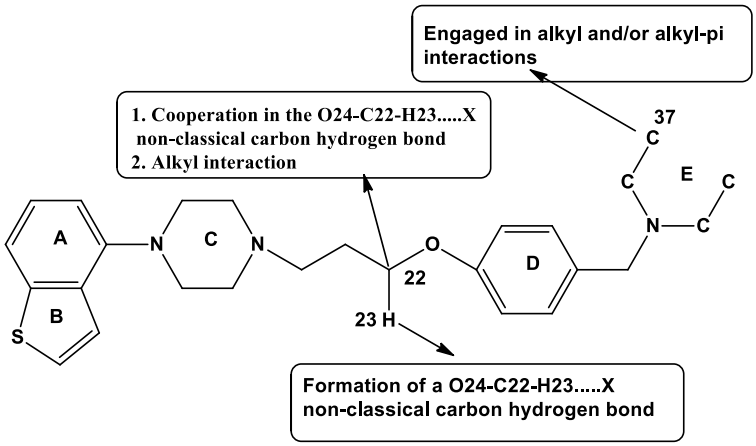

Figure 28: Partial 2D pharmacophore for 5-HT$_{2A}$ receptor affinity

Discussion of the results for the D$_2$ receptor affinity

Table 6 shows that the importance of variables in Eq. 4 is S_{37}^N(LUMO+1)*>> S_{12}^N(LUMO+2)*>> η_{22}*> S_{20}^N(LUMO+2)*. A high D$_2$ receptor affinity is associated with high positive values for S_{37}^N(LUMO+1)*, S_{12}^N(LUMO+2)*, S_{20}^N(LUMO+2)* and η_{22}*.

Atom 37 is a sp^3 carbon atom in ring E (see Fig. 1 and Fig. 10). Table 12 shows that all local MOs have a sigma nature. High positive numerical values for S_{37}^N(LUMO+1)* are obtained by lowering the corresponding eigenvalue, making this local MO more predisposed to interact with electron-rich regions. Therefore, we suggest that atom 37 could be engaged in alkyl and/or alkyl-π interactions.

Atom 12 is a sp^3 carbon atom in ring C (see Fig. 10). Table 10 shows that all local MOs have a sigma nature. A high D$_2$ receptor affinity is associated with high positive values for S_{12}^N(LUMO+2)*. Note that (HOMO)$_{12}$* coincides with the molecular HOMO in all cases (Table 10). The case of (LUMO)$_{12}$* is different: in some cases it coincides with the molecular LUMO but in others it is energetically very far from that MO. To get higher positive numerical values for S_{12}^N(LUMO+2)* we need to diminish the numerical value of (LUMO+2)$_{12}^*$. Therefore, the best situation is when the three lowest empty local MOs coincide with the equivalent molecular MOs. This suggests that atom 12 is close to an electron-rich center. Therefore, probable interactions are alkyl and/or alkyl-π ones (both at a distance of 5.5Å).

Atom 22 is a sp^3 carbon atom in the chain linking rings C and D (see Fig. 10). All local molecular orbitals have a sigma character (Table 11). A high D$_2$ receptor affinity is associated with high numerical values for the local atomic hardness (the (HOMO)$_{22}$*-(LUMO)$_{22}$* energy gap). The local atomic hardness has always-positive numerical values for this kind of molecules. Table 11 shows that in some cases local (HOMO)$_{22}$* coincides with occupied MOs close to the molecular HOMO and in other cases with occupied molecular MOs energetically far from the occupied frontier MO. The (LUMO)$_{22}$* is energetically far from the molecule's LUMO in all cases. The fastest way to obtain large positive numerical values is by changing (HOMO)$_{22}$* in such a way that corresponds to an inner occupied molecular MO. This modification transforms atom 22 in a bad donor and a bad electron acceptor, suggesting that it could be engaged in an alkyl interaction.

Atom 20 is a hydrogen atom bonded to C19 (see Fig. 10). Note that C19 is bonded to N14. All local MOs have a sigma nature (Table 10). A high D$_2$ receptor affinity is associated with high positive numerical values for S_{20}^N(LUMO+2)*. These values are obtained by lowering the corresponding eigenvalue, making this MO more prone to interact with electron-rich centers. Chemically speaking, the best situation is when the three lowest empty MOs of the molecules have a degree of localization on atom 20. We suggest that atom 20 is engaged in a N14-C19-H20.....X non-classical carbon hydrogen bond, where X could be for example oxygen or nitrogen atoms. All the suggestions are displayed in the partial 2D pharmacophore of Fig. 29.

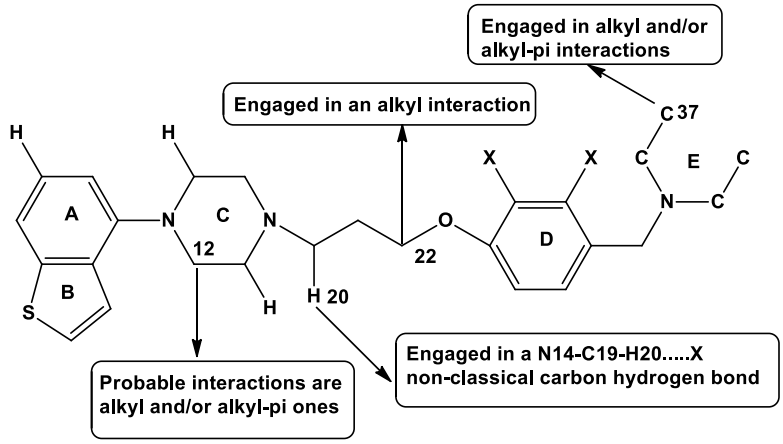

Figure 29: Partial 2D pharmacophore for D_2 receptor affinity

Discussion of the results for the H_3 receptor affinity

Table 8 shows that the importance of variables in Eq. 5 is S_{39}^{N}(LUMO+2)*>> S_{37}^{E}(HOMO-2)*> S_{13}^{N}(LUMO+1)*> S_{34}^{E}(HOMO)*. A high H_3 receptor affinity is associated with high positive numerical values for S_{39}^{N}(LUMO+2)*, with small negative numerical values for S_{37}^{E}(HOMO-2)* and S_{34}^{E}(HOMO)* and with high positive numerical values for S_{13}^{N}(LUMO+1)*.

Atom 39 is a sp^3 carbon atom in ring E (see Fig. 10). All local MOs have a sigma nature (Table 12). Table 12 also shows that in a group of molecules $(HOMO)_{39}$* and $(LUMO)_{39}$* are energetically far from the corresponding molecular frontier MOs. In another group of molecules, $(HOMO)_{39}$* is coincident with the molecule's (HOMO-1) or (HOMO-2), and $(LUMO)_{39}$* is energetically far from the molecular LUMO (i.e., it corresponds to a high empty molecular MO). A high H_3 receptor affinity is associated with high positive numerical values for S_{39}^{N}(LUMO+2)*. Let us remember that:

$$S_{39}^{N}(\text{LUMO+2})^{*}=\frac{F_{39}(\text{LUMO+2})^{*}}{E_{(\text{LUMO+2})_{39}^{*}}} \tag{8}$$

From a mathematical point of view, Eq. 8 shows that high positive numerical values can be obtained by shifting downwards the MO energy. This approach will shift toward zero the energies of $(LUMO)_{39}$* and $(LUMO+1)_{39}$*. This will make these three local MOs more reactive, suggesting that atom 30 is close to an electron-rich center. From the chemist's point of view the ideal situation occurs when the three lowest empty local MOs coincide with the three lowest empty molecular MOs. Possible interactions of atom 39 are alkyl and/or alkyl-π ones.

Atom 34 is a sp3 carbon atom bonded to ring D (see Fig. 10). All local MOs have a sigma nature (Table 12). $(HOMO)_{34}$* is energetically close to the molecular HOMO. $(LUMO)_{34}$* is energetically close to the molecular LUMO (Table 12). A high receptor affinity is associated with small negative numerical values for S_{34}^{E}(HOMO)*. Remembering that:

$$S_{34}^{E}(\text{HOMO})^{*}=\frac{F_{34}(\text{HOMO})_{34}^{*}}{E_{\text{HOMO}_{34}^{*}}} \tag{9}$$

we see that the small negative values are obtained by increasing the MO energy, i.e., making this MO less reactive. Therefore, we need to avoid that the highest occupied molecular MOs be localized on this atom. This atom will become a bad electron donor and prone to interact with electron-rich areas. Like in the case of atom 39, possible interactions of atom 34 are alkyl and/or alkyl-π ones.

Atom 37 is a sp^3 carbon atom in ring E (see Fig. 10). Table 12 shows that all local MOs have a sigma nature. A high histamine H_3 receptor affinity is associated with small negative numerical values for S_{37}^{E}(HOMO-2)*. The only mode to get small negative numerical values is by removing the localization of the three highest occupied molecular MOs on atom 37. All this procedure will make C37 a bad electron donor. For this reason, we suggest that this atom could be engaged in alkyl and/or alkyl-π interactions.

Atom 13 is a sp^3 carbon atom in ring C (see Fig. 10). All local MOs have a sigma nature (Table 10). A high receptor affinity is associated with high positive numerical values for S_{13}^{N}(LUMO+1)*. To get the high positive numerical values we must shift toward zero the $(LUMO+1)_{13}$* energy, making it more reactive. Therefore, the ideal situation occurs when at least the two lowest empty local MOs coincide with the two lowest empty molecular MOs. Possible interactions of atom 13 are alkyl and/or alkyl-π ones. All the suggestions are displayed in the partial 2D pharmacophore of Fig. 30.

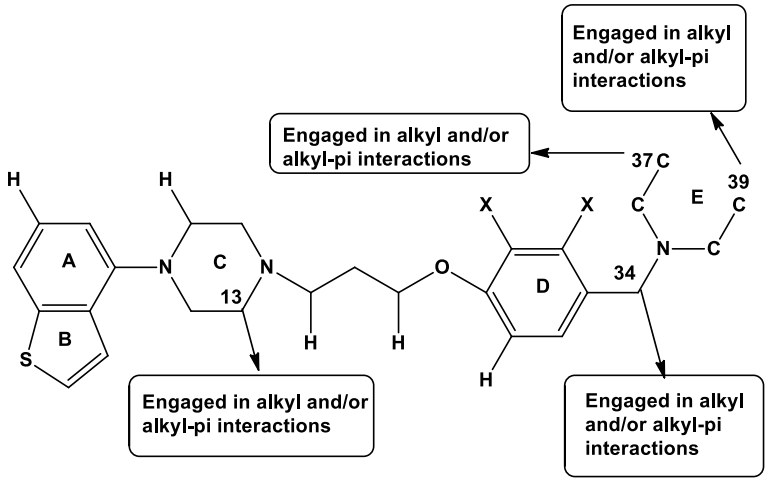

Figure 30: Partial 2D pharmacophore for H_3 receptor affinity

Finally, we shall present some comments about geometry optimization and molecular electrostatic potential (MEP) maps.

The geometry optimization was carried out in the presence of water, simulated with one of the methods available in Gaussian 16. Water is used because the experiments to obtain the IC_{50} were done in an aqueous medium, so this calculation allows us to see a possible conformation of the molecules in said environment. To show some of the results obtained, we have selected molecules 22 and 9, which are, respectively, those with the highest and lowest affinity for the serotonin 5-HT_{2A} receptor.

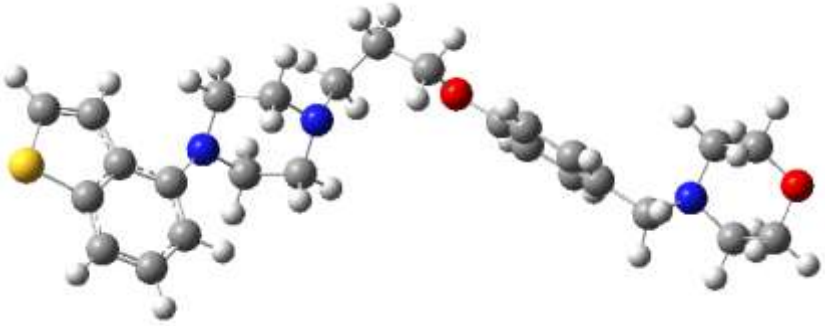

Figure 31: Final geometry of molecule 22

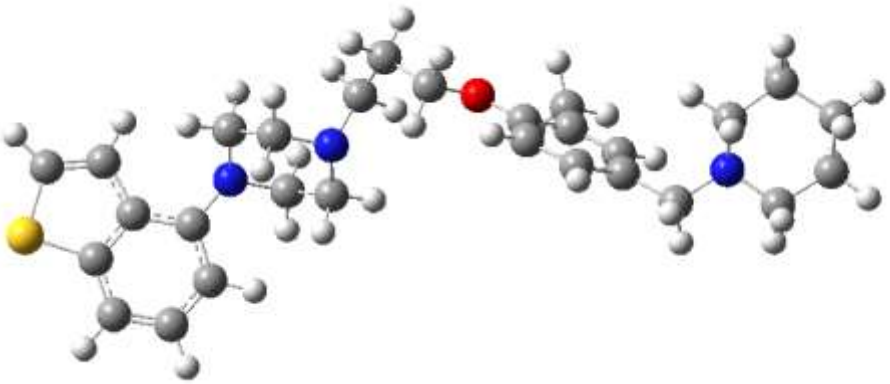

Figure 32: Final geometry of molecule 9

The rest of the molecules have a more or less similar conformation. These results are shown because it is important to highlight that the conformation itself is not a datum that allows establishing relations between the structure and the activity.

The molecular electrostatic potential (MEP) map shows the force of attraction or repulsion felt by a positive point charge (proton) at various points in space that are equidistant from a molecular surface. It is then possible to interpret it as a map of regions of electron excess and electron deficiency. In general, the receptors can be located on the surface or inside the passageways of macromolecules. What can be stated is that, whatever this location, the drug molecule must follow a path that leads it to interact with the receptor. For that reason, it is conceivable to assume that the MEPs of the various molecules must be more or less similar in order to interact with the various molecular species in a similar way in the aforementioned pathway. In figures 33 and 34, we show the MEP map of molecules 22 and 9 (made with GaussView).

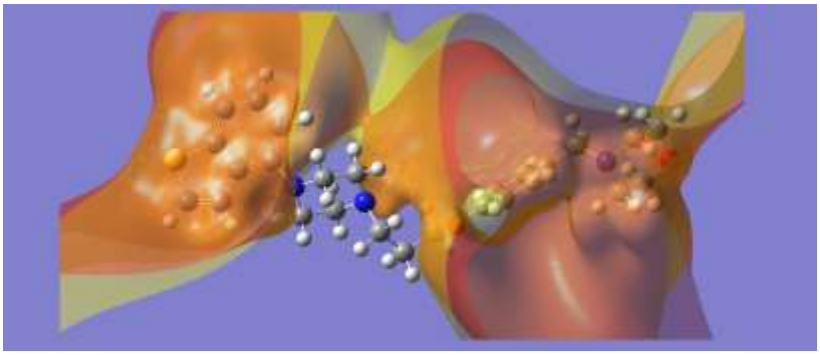

Figure 33: MEP map of molecule 22 (isovalue of -0.0004 in orange and +0.0004 in yellow)

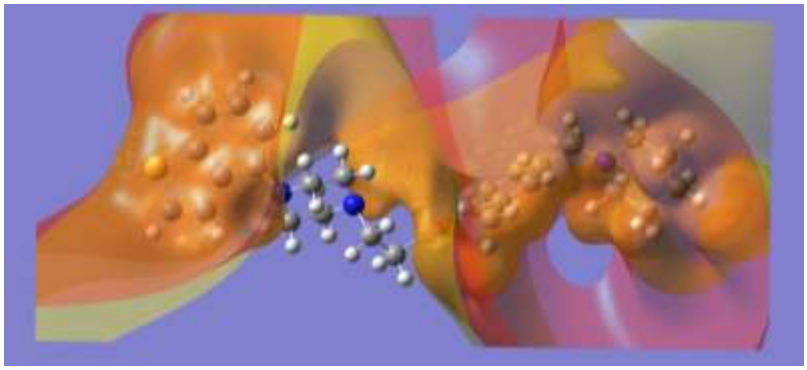

Figure 34: MEP map of molecule 9 (isovalue of -0.0004 in orange and +0.0004 in yellow)

At this short distance, the possible drug-receptor interactions would be of the hydrogen bond type, halogen type and/or π-lone pair interactions.

It is also possible to represent the MEP as a surface located at a certain distance from the nuclei. As an example, in figures 35 and 36 we show the PEM of molecules 22 and 9 at a distance of 4.5Å from the nuclei (made with Molekel).

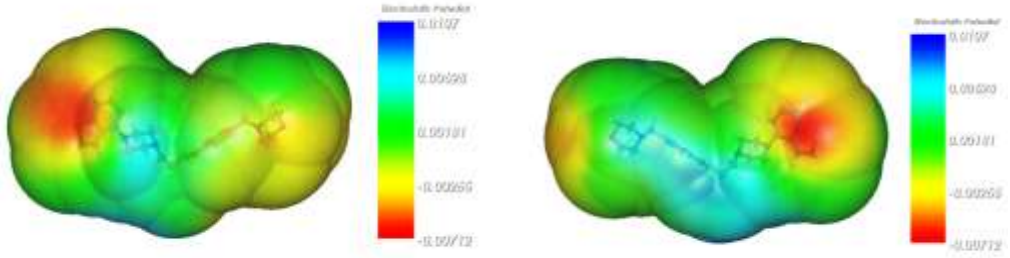

Figure 35: MEP surface of molecule 22 at 4.5Å from the nuclei. Front view (left) and rear view (right)

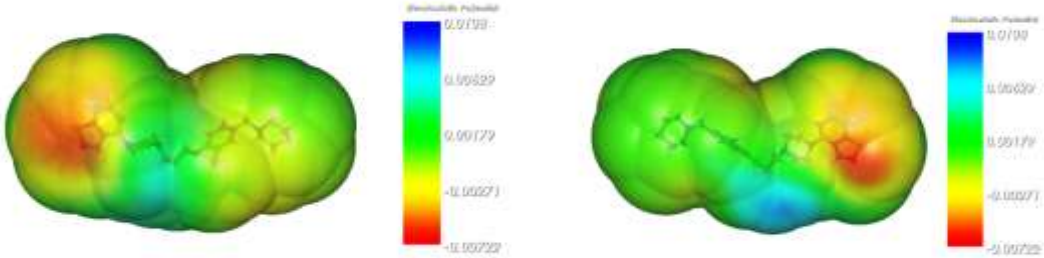

Figure 36: MEP surface of molecule 9 at 4.5Å from the nuclei. Front view (left) and rear view (right).

It can be seen that, in a qualitative and general way, the MEP maps of both molecules are similar. At this distance, some interactions with the receptor are already possible, such as π-cation (5Å), π-anion (5Å), π-σ (4.1Å) and π-S (4.5Å). In figures 37 and 38, we show the MEP of molecules 22 and 9 at a distance of 6Å from the nuclei.

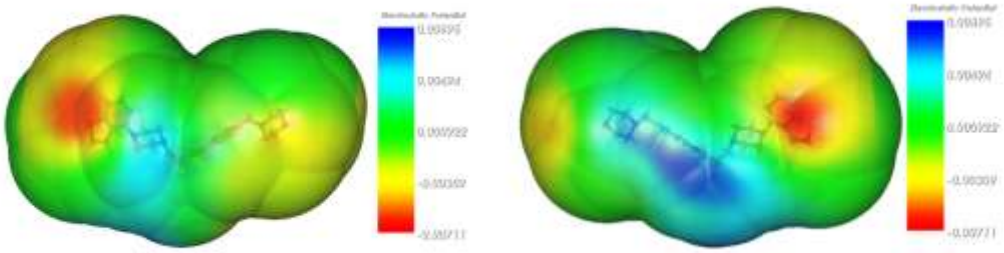

Figure 37: MEP surface of molecule 22 at 6Å from the nuclei. Front view (left) and rear view (right)

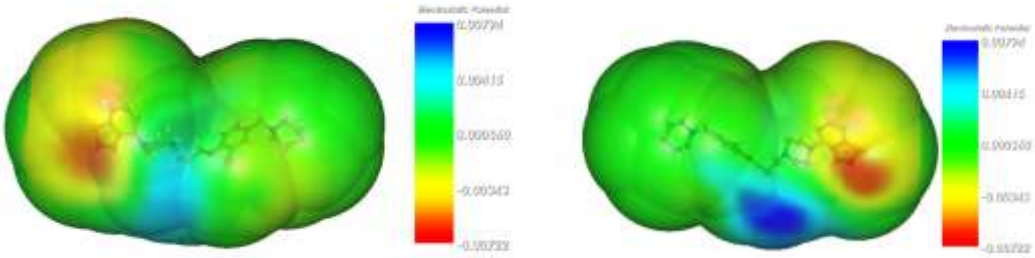

Figure 38: MEP surface of molecule 9 at 6Å from the nuclei. Front view (left) and rear view (right)

It can be seen that, in a qualitative and general way, the MEPs of both molecules are similar. At this distance, possible drug-receptor interactions of the π-π, amide-π and alkyl (between aliphatic chains) type may exist.

In summary, the results obtained support the hypothesis tested in this work and should help experimentalists to design new molecules with enhanced activity. A large number of studies also support the hypothesis that the linear form of the KPG method is enough to get good QSAR results. Nevertheless, and from a philosophical point of view, there is always the possibility that a group of biological activity results cannot be explained by the linear form of the KPG method. This is one of the pleasures of scientific research.

References

[1]. Shrivastava, A.; De Sousa, A. *Schizophrenia treatment outcomes: An evidence-based approach to recovery*. Springer Nature: Switzerland, 2020.

[2]. Correll, C. U.; Schooler, N. R. Negative Symptoms in Schizophrenia: A Review and Clinical Guide for Recognition, Assessment, and Treatment. *Neuropsychiatric Disease and Treatment* 2020, 16, 519-534.

[3]. Smart, S.; Kępińska, A.; Murray, R.; MacCabe, J. Predictors of treatment resistant schizophrenia: a systematic review of prospective observational studies. *Psychological Medicine* 2021, 51, 44-53.

[4]. Siskind, D.; Orr, S.; Sinha, S.; Yu, O.; Brijball, B.; Warren, N.; MacCabe, J. H.; Smart, S. E.; Kisely, S. Rates of treatment-resistant schizophrenia from first-episode cohorts: systematic review and meta-analysis. *The British Journal of Psychiatry* 2021, 1-6.

[5]. Rouy, M.; Saliou, P.; Nalborczyk, L.; Pereira, M.; Roux, P.; Faivre, N. Systematic review and meta-analysis of metacognitive abilities in individuals with schizophrenia spectrum disorders. *Neuroscience & Biobehavioral Reviews* 2021, 126, 329-337.

[6]. Legge, S. E.; Santoro, M. L.; Periyasamy, S.; Okewole, A.; Arsalan, A.; Kowalec, K. Genetic architecture of schizophrenia: a review of major advancements. *Psychological Medicine* 2021, 51, 2168-2177.

[7]. Huxley, P.; Krayer, A.; Poole, R.; Prendergast, L.; Aryal, S.; Warner, R. Schizophrenia outcomes in the 21st century: A systematic review. *Brain and Behavior* 2021, 11, e02172.

[8]. Horne, C. M.; Vanes, L. D.; Verneuil, T.; Mouchlianitis, E.; Szentgyorgyi, T.; Averbeck, B.; Leech, R.; Moran, R. J.; Shergill, S. S. Cognitive control network connectivity differentially disrupted in treatment resistant schizophrenia. *NeuroImage: Clinical* 2021, 30, 102631.

[9]. Hannon, E.; Dempster, E. L.; Mansell, G.; Burrage, J.; Bass, N.; Bohlken, M. M.; Corvin, A.; Curtis, C. J.; Dempster, D.; Di Forti, M. DNA methylation meta-analysis reveals cellular alterations in psychosis and markers of treatment-resistant schizophrenia. *Elife* 2021, 10, e58430.

[10]. Crespo-Facorro, B.; Such, P.; Nylander, A.-G.; Madera, J.; Resemann, H. K.; Worthington, E.; O'Connor, M.; Drane, E.; Steeves, S.; Newton, R. The burden of disease in early schizophrenia–a systematic literature review. *Current Medical Research and Opinion* 2021, 37, 109-121.

[11]. Citrome, L.; Volavka, J. Specific anti-hostility effects of atypical antipsychotics in persons with schizophrenia: from clozapine to cariprazine. *Harvard Review of Psychiatry* 2021, 29, 20-34.

[12]. Gomes, F. V.; Grace, A. A. Beyond dopamine receptor antagonism: new targets for schizophrenia treatment and prevention. *International Journal of Molecular Sciences* 2021, 22, 18.

[13]. Gross, G.; Geyer, M. A. *Current Antipsychotics*. Springer Science & Business Media: 2012; Vol. 212.

[14]. Remington, G. Second and Third Generation Antipsychotics. In *Encyclopedia of Psychopharmacology*, Stolerman, I. P., Ed. Springer Berlin Heidelberg: Berlin, Heidelberg, 2010; pp 1187-1192.

[15]. Gardner, D. M.; Teehan, M. D. *Antipsychotics and their side effects*. Cambridge University Press: New York, 2010.

[16]. Stępnicki, P.; Kondej, M.; Koszła, O.; Żuk, J.; Kaczor, A. A. Multi-targeted drug design strategies for the treatment of schizophrenia. *Expert Opinion on Drug Discovery* 2021, 16, 101-114.

[17]. Gao, L.; Hao, C.; Ma, R.; Chen, J.; Zhang, G.; Chen, Y. Synthesis and biological evaluation of a new class of multi-target heterocycle piperazine derivatives as potential antipsychotics. *RSC Advances* 2021, 11, 16931-16941.

[18]. Gao, L.; Hao, C.; Chen, J.; Ma, R.; Zheng, L.; Wu, Q.; Liu, X.; Liu, B.-F.; Zhang, G.; Chen, Y. Discovery of a new class of multi-target heterocycle piperidine derivatives as potential antipsychotics with pro-cognitive effect. *Bioorganic & Medicinal Chemistry Letters* 2021, 40, 127909.

[19]. Chen, Y.; Lan, Y.; Wang, S.; Zhang, H.; Xu, X.; Liu, X.; Yu, M.; Liu, B.-F.; Zhang, G. Synthesis and evaluation of new coumarin derivatives as potential atypical antipsychotics. *European Journal of Medicinal Chemistry* 2014, 74, 427-439.

[20]. McRobb, F. M.; Crosby, I. T.; Yuriev, E.; Lane, J. R.; Capuano, B. Homobivalent ligands of the atypical antipsychotic clozapine: design, synthesis, and pharmacological evaluation. *Journal of Medicinal Chemistry* 2012, 55, 1622-1634.

[21]. Capuano, B.; Crosby, I. T.; McRobb, F. M.; Podloucka, A.; Taylor, D. A.; Vom, A.; Yuriev, E. The Synthesis and Preliminary Pharmacological Evaluation of a Series of Substituted 4′-Phenoxypropyl Analogues of the Atypical Antipsychotic Clozapine. *Australian Journal of Chemistry* 2010, 63, 116-124.

[22]. Capuano, B.; Crosby, I. T.; Lloyd, E. J.; Neve, J. E.; Taylor, D. A. Aminimides as potential CNS acting agents. I. Design, synthesis, and receptor binding of 4′-aryl aminimide analogues of clozapine as prospective novel antipsychotics. *Australian Journal of Chemistry* 2007, 60, 673-684.

[23]. The results presented here are obtained from what is now a routinary procedure. For this reason, all papers have a similar general structure. This model contains *standard* phrases for the presentation of the methods, calculations and results because they do not need to be rewritten repeatedly and because the number of possible variations to use is finite. See: Hall, S., Moskovitz, C., and Pemberton, M. 2021. Understanding Text Recycling: A Guide for Researchers. Text Recycling Research Project. Online at textrecycling.org.

[24]. Gómez-Jeria, J. S. 45 Years of the KPG Method: A Tribute to Federico Peradejordi. *Journal of Computational Methods in Molecular Design* 2017, 7, 17-37.

[25]. Gómez-Jeria, J. S. A New Set of Local Reactivity Indices within the Hartree-Fock-Roothaan and Density Functional Theory Frameworks. *Canadian Chemical Transactions* 2013, 1, 25-55.

[26]. Gómez-Jeria, J. S.; Robles-Navarro, A.; Kpotin, G.; Garrido-Sáez, N.; Gatica-Díaz, N. Some remarks about the relationships between the common skeleton concept within the Klopman-Peradejordi-Gómez QSAR method and the weak molecule-site interactions. *Chemistry Research Journal* 2020, 5, 32-52.

[27]. Gómez-Jeria, J. S.; Ibertti-Arancibia, A.; Olarte-Lezcano, L. A theoretical study of the relationships between electronic structure of 2-aryladenine derivatives and percentage of inhibition of radioligand binding in human A_{2A} and A_{2B} adenosine receptors. *Chemistry Research Journal* 2022, 7, 1-18.

[28]. Gómez-Jeria, J. S.; Silva-Monroy, S. A quantum-chemical analysis of the relationships between electronic structure and inhibition of SARS-CoV-2 virus by a group of cyclic sulfonamide derivatives. *Chemistry Research Journal* 2021, 6, 54-70.

[29]. Gómez-Jeria, J. S.; Robles-Navarro, A.; Soza-Cornejo, C. A note on the relationships between electronic structure and serotonin 5-HT_{1A} receptor binding affinity in a series of 4-butyl-arylpiperazine-3-(1*H*-indol-3-yl)pyrrolidine-2,5-dione derivatives. *Chemistry Research Journal* 2021, 6, 76-88.

[30]. Gómez-Jeria, J. S.; Robles-Navarro, A.; Soto-Martínez, V. Quantum Chemical Analysis of the relationships between electronic structure and dopamine D_1 and D_5 receptor binding affinities in a series of 1-phenylbenzazepines. *Chemistry Research Journal* 2021, 6, 128-144.

[31]. Gómez-Jeria, J. S.; Ibertti-Arancibia, A. A DFT study of the relationships between electronic structure and dopamine D_1 and D_2 receptor affinity of a group of (S)-enantiomers of 11-(1,6-dimethyl-1,2,3,6-tetrahydropyridin-4-yl)-5*H*-dibenzo[b,e][1,4] diazepines. *Chemistry Research Journal* 2021, 6, 116-131.

[32]. Gómez-Jeria, J. S.; Crisóstomo-Cáceres, S. R.; Robles-Navarro, A. On the compatibility between formal QSAR results and docking results: the relationship between electronic structure and H5N1 (A/goose/Guangdong/SH7/2013) neuraminidase inhibition by some Tamiflu derivatives as an example. *Chemistry Research Journal* 2021, 6, 46-59.

[33]. Gómez-Jeria, J. S.; Sotomayor, P. Quantum chemical study of electronic structure and receptor binding in opiates. *Journal of Molecular Structure: THEOCHEM* 1988, 166, 493-498.

[34]. Gómez-Jeria, J. S.; Morales-Lagos, D.; Rodriguez-Gatica, J. I.; Saavedra-Aguilar, J. C. Quantum-chemical study of the relation between electronic structure and pA2 in a series of 5-substituted tryptamines. *International Journal of Quantum Chemistry* 1985, 28, 421-428.

[35]. Gómez-Jeria, J. S.; Morales-Lagos, D. R. Quantum chemical approach to the relationship between molecular structure and serotonin receptor binding affinity. *Journal of Pharmaceutical Sciences* 1984, 73, 1725-1728.

[36]. Gómez-Jeria, J. S.; Espinoza, L. Quantum-chemical studies on acetylcholinesterasa inhibition. I. Carbamates. *Journal of the Chilean Chemical Society* 1982, 27, 142-144.

[37]. Frisch, M. J.; Trucks, G. W.; Schlegel, H. B.; Scuseria, G. E.; Robb, M. A.; Cheeseman, J. R.; Scalmani, G.; Barone, V.; Petersson, G. A.; Nakatsuji, H.; Li, X.; Caricato, M.; Marenich, A. V.; Bloino, J.; Janesko, B. G.; Gomperts, R.; Mennucci, B.; Hratchian, H. P. *Gaussian 16 Rev. A.03*, Gaussian: Pittsburgh, PA, USA, 2016.

[38]. Gómez-Jeria, J. S. *D-Cent-QSAR: A program to generate Local Atomic Reactivity Indices from Gaussian16 log files*, v. 1.0; Santiago, Chile, 2020.

[39]. Gómez-Jeria, J. S. An empirical way to correct some drawbacks of Mulliken Population Analysis (Erratum in: J. Chil. Chem. Soc., 55, 4, IX, 2010). *Journal of the Chilean Chemical Society* 2009, 54, 482-485.

[40]. Statsoft. *Statistica v. 8.0*, 2300 East 14 th St. Tulsa, OK 74104, USA, 1984-2007.